

## EARLY PRODUCTS OF PYROLYSIS OF WOOD

William F. DeGroot, Wei-Ping Pan, M. Dalilur Rahman, Geoffrey N. Richards

Wood Chemistry Laboratory, University of Montana, Missoula, Montana 59812 USA

### INTRODUCTION

We are studying the first stages in pyrolysis of wood and other cellulosic materials as part of a study of the chemistry of smoldering or low-temperature combustion. In the latter processes both oxidative and non-oxidative pyrolysis occur. This paper describes an investigation of the first volatile products of pyrolysis of wood and we believe that many of the conclusions regarding the first pyrolysis reactions at low temperatures are applicable also to higher temperature treatments of wood such as are utilized in liquifaction processes. Our aim was primarily to determine the relative rates and modes of pyrolysis of the three major constituents of wood (viz. cellulose, hemicelluloses and lignin) from their chemically intact situation in whole wood. We believe that interactions of these substances and of their degradation products during pyrolysis make this approach necessary and may invalidate some aspects of earlier studies of pyrolysis of isolated wood fractions.

### METHODS

Our major technique has been the coupling of a thermogravimetric analysis system (TG) with a Fourier transform infrared spectrometer. The coupling is by a heated 1 m. teflon tube from the TG to an infrared gas cell. All of the results were obtained with cottonwood sapwood (*Populus trichocarpa*) which had been ground to pass an 80 mesh sieve. All pyrolyses were carried out in flowing nitrogen, the time lag between the thermal balance and the gas cell was 1 min, and heating was either isothermal at 250°C or at 3°/min. from 100° to 500°. In the isothermal runs for periods up to 2 hrs. the whole infrared spectrum could be accounted for by the absorption bands of the 6 components shown in Table 1. The system was therefore calibrated for these compounds by heating the pure liquid in a loosely covered pan on the thermal balance at an appropriate temperature and relating the rate of weight loss to the infrared spectrum. Where a wavenumber range is shown in Table 1, the absorbance was integrated between these values and where a single wavenumber is given, the height of that Q branch was used. These values bore a linear relationship to the rate of weight loss for an individual compound, and the resultant calculated response factors were used to calculate the rates of production of each product from heated wood samples. For carbon dioxide the calibration was based on air versus a pure nitrogen blank and the carbon monoxide calibration was then deduced from a standard mixture of the two oxides in nitrogen.

The effects of cations on the pyrolyses were investigated with wood which had been washed with acid to remove all metal ions and with samples in which the indigenous cations had been replaced entirely with either potassium or calcium ions. These ion exchange processes caused no other chemical change in the wood. E.g. the content of L-arabinofuranose units (which comprise one of the most acid-labile groups in wood) was unchanged.

Total absolute glucose contents of the wood samples were determined by acid hydrolysis, reduction, acetylation and gas chromatography using i-inositol as internal standard (1). Uronic acids were determined on a aliquot portion of the hydrolyzates (2) and vanillin and syringaldehyde from lignin were generated by nitrobenzene oxidation (3) and determined by gas chromatography of trimethylsilyl ethers. The glucan components of the heated wood samples were very resistant to hydrolysis with 72% sulfuric acid and it was necessary to "reactivate" with water before hydrolysis.

## RESULTS AND DISCUSSION

Figure 1 shows that the cations have a major influence on the rate of pyrolysis of wood. The results confirm earlier studies (4) and show that of the two major cations present in wood, potassium is dominant in catalysis of pyrolysis, whereas calcium tends to stabilize the wood towards pyrolysis. The low temperature inflection in the DTG curves at 250-300° has often been assumed to be associated with hemicellulose and/or lignin degradation and since the cations occur predominantly in the hemicelluloses (5) we have studied pyrolysis in this region in some detail by isothermal pyrolysis at 250°. Figure 2 shows the weight loss under such conditions and the rates of weight loss for original wood and for potassium-exchanged wood were indistinguishable. The weight loss curves for acid-washed and for calcium-exchanged wood were also indistinguishable, but corresponded to a much lower rate of pyrolysis.

The rates of formation of the volatile products determined by infrared spectroscopy are shown in Figure 3 for the original wood. Similar results are also available for the ion-exchanged woods. Table 2 shows the proportion of total weight loss in the wood sample that can be accounted for by the infrared analysis. The 40% of unaccounted weight loss represents material which condensed before reaching the infrared cell. This is likely to consist of a mixture of larger molecules containing two or more carbon atoms. It is evident that carbon dioxide and methanol are the first products of pyrolysis at 250°, very closely followed by water, which is the major product on either a weight or molar basis. Formic acid is produced steadily over a relatively long period, while acetic acid production peaks much later than the carbon dioxide, methanol and water. The changes in glycose, uronic acid, vanillin and syringaldehyde content are shown in Table 3. We conclude that the methanol is formed predominantly by pyrolysis of lignin with syringyl units pyrolysing rather more rapidly than guaiacyl. The amount of methanol released is much greater than could be accounted for by the 4-O-methylglucuronic acid units of the hemicelluloses. Evidently however, some units or regions of the lignin are especially labile; only about half of the available methanol is released in 1 hr. at 250°, possibly in two stages, and the remainder requires higher temperatures (see below). The carbon dioxide is evidently derived predominantly from decarboxylation of uronic acids which decrease rapidly in the solid residue and the molar yield of carbon dioxide corresponds approximately with the uronic acid content of the wood. Since the glucan content of the wood is virtually unchanged in 50 min. at 250°, it appears that cellulose survives this treatment, although it is quite likely that some chain scission will occur and perhaps some transglucosylation. The acetic acid is almost certainly released by pyrolysis of the acetyl ester groups from the xylan and its yield is approximately that anticipated from the acetyl content of the wood.

The water, which is the major product, must be formed predominantly from the hemicelluloses. Some water will obviously be formed from the uronic acid and arabinose units which decompose rapidly, but water must also be derived from xylose units which show some decrease. Since we would anticipate that the  $\beta$ -1,4-xylan chain should have a thermal stability similar to cellulose and since glucose does not decrease, it seems probable that some of the xylose units may be subject to rapid elimination reactions yielding water, particularly in the regions of the hemicellulose molecules in which uronic acids are decomposing. The pyrolysis of acetyl ester groups might also be associated with decomposition of the attached xylose units.

The mechanism of formic acid formation is not known. It could be derived from either hemicelluloses or lignin, although by analogy with its formation from polysaccharides by alkali degradation, the former seem more likely.

The influences of cations on yields of carbon dioxide, carbon monoxide (formed above 250°), methanol and formic acid during pyrolysis at temperatures up to 400° are shown in Figures 4-7. The yields of water and acetic acid were much less

sensitive to cation variation and are not shown. Figure 4 shows that the potassium ions favor increased formation of carbon dioxide and lower the temperature of peak production compared with the acid-washed or calcium forms. The total yield of carbon dioxide is much greater than could be explained by decarboxylation of uronic acids alone. The mechanism of formation of this carbon dioxide is not known. Since the bulk of the carbon dioxide is formed above 300° it must be derived at least partly from cellulose. Carbon monoxide was not significantly formed at 250°, but was produced in similar molar amount to carbon dioxide at higher temperatures, peaking at about 350° (Figure 7). It seems probable that this product also is largely produced from cellulose.

The formation of methanol (Figure 5) shows a distinct second peak at about 300° for original and for potassium-exchanged wood. Presumably the methanol evolved above 320° is catalyzed by potassium and derived by pyrolysis reactions from the more resistant lignin which survives pyrolysis at lower temperatures. Formic acid (Figure 6) evidently forms at higher temperatures by potassium catalyzed pyrolysis reactions from cellulose. The same acid is a major product of alkaline degradation of cellulose in absence of air and it is probable that the greater effectiveness of potassium compared with calcium in catalyzing formation of formic acid (and perhaps methanol) is associated with the greater basicity of the former.

#### REFERENCES

1. E.g., M.J. Neilson and G.N. Richards, Carbohydr. Res. 104 (1982) 121-138.
2. N. Blumenkrantz and G. Asboe-Hansen, Anal. Biochem., 54 (1973) 484-489.
3. B. Leopold and I.L. Malmstrom, Acta Chem. Scand., 6 (1952) 49-55.
4. W.F. DeGroot and F. Shafizadeh, J. Anal. Appl. Pyrol., 6 (1984) 217-232.
5. W.F. DeGroot, Carbohydr. Res., 142 (1985) 172-178.

Table 1. Infrared absorbances used to quantify the first volatile products from pyrolysis of wood and conditions used for calibration.

Compound	Wavenumbers (cm <sup>-1</sup> )	Temperature (°C)	Rate of Weight Loss (µg/min)
CO <sub>2</sub>	2240 - 2400	--	
CO	2020 - 2240	--	
CH <sub>3</sub> COOH	1140 - 1230	23, 30	16, 32
H <sub>2</sub> O	1653	23, 30	17, 61
HCOOH	1105	23, 26	12.6, 30.0
CH <sub>3</sub> OH	1032	23, 30	42.6, 137

Table 2. Yield of volatile products by infrared detection as percentage of total weight loss; cottonwood at 250°C in nitrogen.

	<u>% of Total Weight Loss</u>			
Methanol	3.5	3.7	3.8	4.4
Formic acid	5.0	6.4	8.2	7.0
Acetic acid	7.5	15.5	19.0	23.0
Carbon dioxide	10.5	9.2	12.0	13.2
Water	<u>21.5</u>	<u>18.3</u>	<u>16.0</u>	<u>13.2</u>
Total	47.5%	53.1%	59.0%	60.8%
Time at 250°	11 min	23 min	40 min	58 min
Total weight loss	5.5%	8.0%	11.0%	12.5%

Table 3. Analyses of cottonwood after heating at 250°C under nitrogen.

Analysis (% dry weight)	Original Dry Wood	250°/N <sub>2</sub> /50 min.
(Anhydroglycoses)		
Rhamnose	0.2	0
Arabinose	0.5	trace
Xylose	15.8	12.3
Mannose	3.0	2.4
Glucose	51.3	51.3
Uronic acid	4.9	1.7
Total Carbohydrate	75.7	67.7
Vanillin	2.7	1.8
Syringaldehyde	5.7	2.2
Weight loss	0	11.9%

FIG. 1  
DTG  
Cottonwood, N<sub>2</sub>, 3°/min.

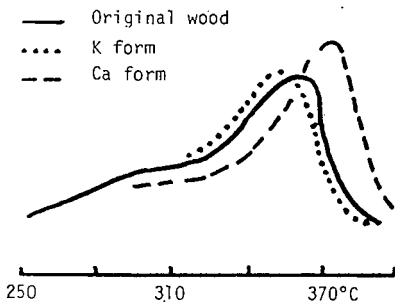
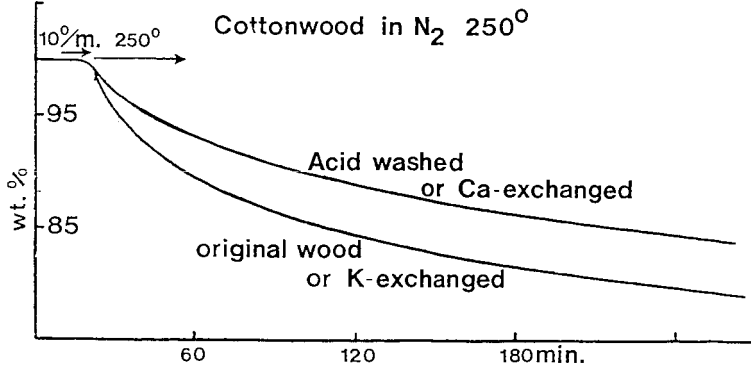
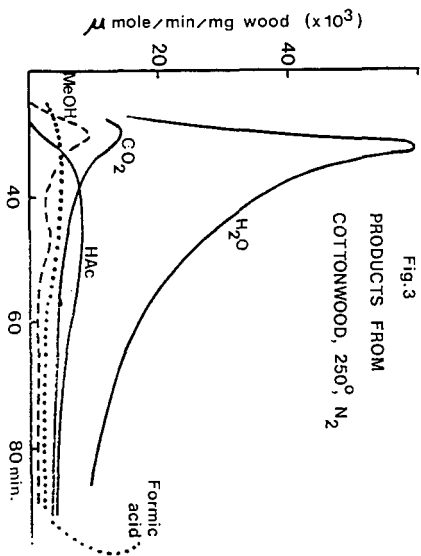
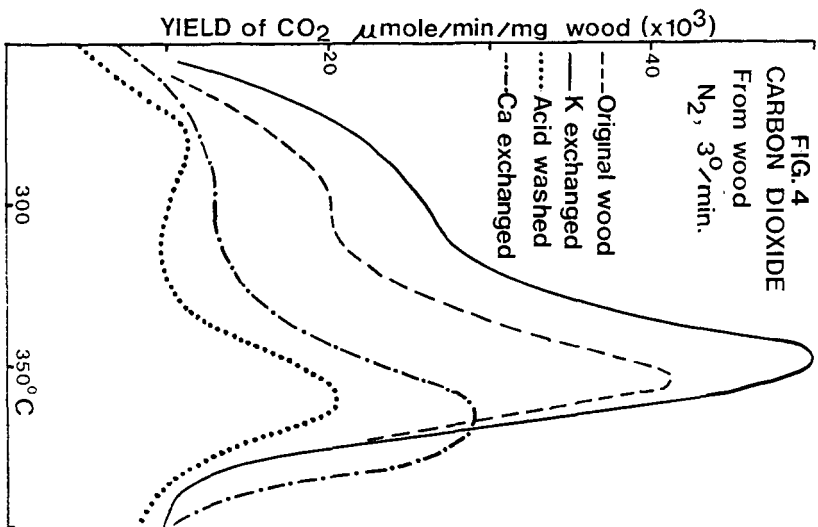
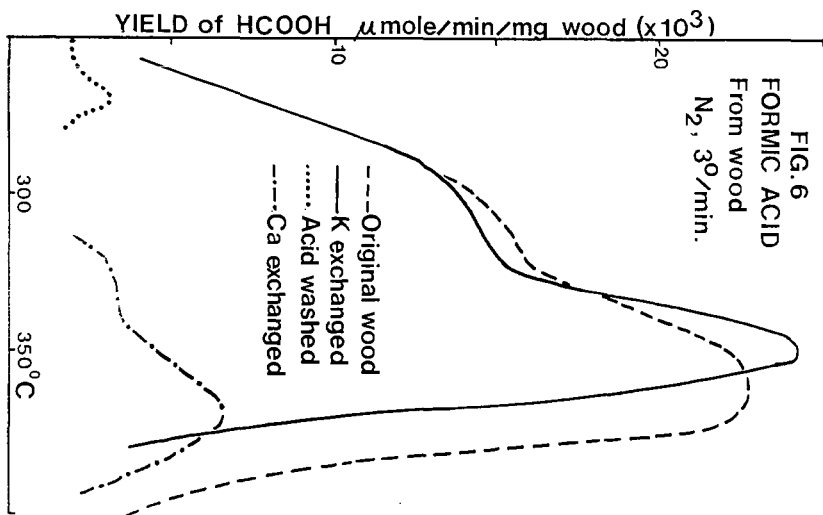
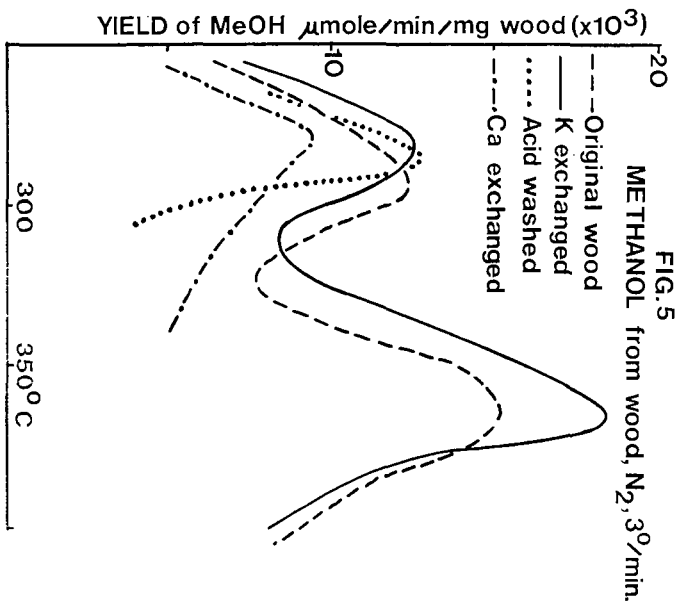
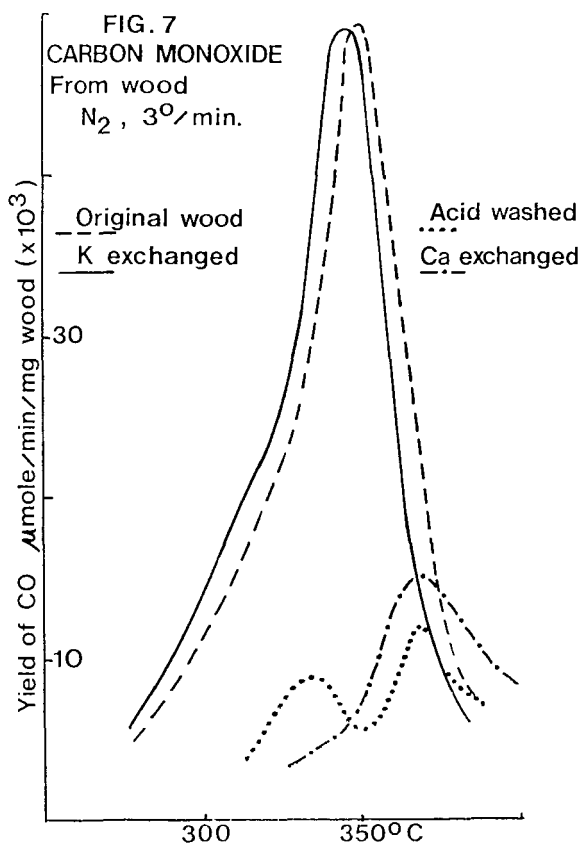


Fig. 2









## Conditions that Favor Tar Production from Pyrolysis of Large, Moist Wood Particles

Marcia Kelbon, Scott Bousman, and Barbara Krieger-Brockett

Dept. of Chemical Engineering, BF-10  
University of Washington  
Seattle, WA 98195

### Abstract

The production of pyrolytic oils from biomass will be greatly facilitated if large, and perhaps moist, particles can be used directly as a feedstock. This paper describes experiments to quantify product evolution rates, as well as spatial and temporal temperature distributions, during pyrolysis of large wood particles. The experiments have been performed using well-defined, reactor-independent conditions which will aid in identifying favorable conditions for tar production from large particles. The experiments reveal that an optimum moisture content can facilitate tar production. The reacted fraction that is tar is greater for intermediate moisture contents, particle sizes, and heating rates, and the optimum tar production conditions for moist feed change with both heating intensity and particle size.

### INTRODUCTION

The economics of making pyrolytic oils from biomass will be improved if large, and perhaps moist, particles can be used directly as a feedstock. This is a result of the high cost of size reduction and drying of fibrous and often green biomass. However, the pyrolysis of realistically sized particles (about 1 x 1 x .5 cm or greater) is complicated by the lack of uniform temperature profiles within the particle, and the synergistic effects that external heating intensity, moisture, and particle size have in altering the intraparticle temperature histories. Nevertheless, both present and planned industrial biomass converters employ large particles, sometimes using them in fluidized beds which are less sensitive to feed size distributions (1).

Selectively producing a particular pyrolysis fraction such as tar, or specific components in any fraction, is difficult. The majority of studies to date have used finely ground (< 100  $\mu\text{m}$  diameter) wood samples in which heat transfer rates are rapid enough to cause a uniform particle temperature, and mass transfer is fast enough to minimize secondary reactions. For these particles, pyrolysis with a high heating rate to moderately high temperatures generally favors tar formation, if the tar can be quickly removed from the reaction zone. However, reducing fibrous materials to such a small size is costly. Pyrolysis feeds are likely to be wood chips used routinely in the forest products industry. In wood chip pyrolysis, the particle interior heats slowly and secondary reactions of tar are significant.

The scope of this preprint is limited to the presentation and discussion of experimental conditions of practical importance that maximize tar from pyrolysis of large wood particles. By design, results are as independent of reactor type to the greatest possible, and reveal the effects of heat and mass transport that are critical to conversion of the large, poorly conducting porous particles. Since typical feeds are heterogeneous, the entity appropriate for chemical engineering studies is the single particle. The findings are then applicable to all reactors in which the chosen experimental conditions prevail. The study of reacting single particles has proven extremely successful in the development of catalytic reactors (2) and coal pyrolysis (3,4,5).

Since reaction temperature is not an independent variable for large pyrolyzing particles, special attention must be given to choosing experimental conditions for the 0.5 cm to 1.5 cm thick

particles studied. Heating intensity can be made precise by controlling the applied heat flux at the particle surface or imposing a surface temperature, and measuring the particle thermal properties (6). One dimensional heating has been used experimentally (7,8) and typifies the type of heat transfer experienced by most wood chips owing to the large aspect ratios they usually have (9). The lowest heating intensity studied,  $2 \text{ cal/cm}^2\text{-s}$ , barely chars thick samples (or causes smoldering combustion if oxygen is present). The highest,  $6 \text{ cal/cm}^2\text{-s}$ , is found in furnaces or high temperature reactors designed for maximum heating of particles. Biomass moisture varies with species and age as well as from region to region. Typical moisture contents (dry basis) found for feed piles in the Pacific Northwest range from 10% to 110%, thus the choices for the experiments reported here. A more complete discussion of practical conditions appears elsewhere (10). Also, simultaneous variations in two or three experimental conditions were systematically investigated in order to determine if pyrolysis tar yields, as well as other reaction products, were dependent on process condition combinations in a non-additive, or multiplicative way (11).

## **EXPERIMENTAL**

**Apparatus** - A description and diagram of the single particle pyrolysis reactor appears in Chan, et al. (12) but a brief presentation is given for completeness. A wood cylinder was placed in a glass sleeve and reactor assembly. An arc lamp provided radiative, spatially uniform, 1-D axial heating as verified by absolute calibration of the heat flux (6,13, 14). The heating period was the same for all experiments, 12 min, sufficiently short to enable the study of active devolatilization in the thinnest of these particles. Thermocouples at 2, 4, and 6 cm from the heated face automatically measured the devolatilization front progress. An infrared pyrometer, mounted off-axis from the arc lamp beam, measured the surface temperature of the pellet. The glass housing and baffle allowed the front face of the pellet to be uniformly irradiated and prevented volatiles from condensing on the window. The large helium carrier gas flowrate quenched the volatiles and swept them without significant backmixing or reaction (6) to the analysis system. The helium pressure on the unheated face was slightly elevated to ensure volatiles flow toward the heated face for maximum recovery. It has been verified (7) that during devolatilization of a large particle, nearly of the volatiles flow toward the heated surface owing to the decreased porosity behind the reaction front. A cold trap (packed with glass wool and at  $-40 \text{ C}$ ) immediately downstream from the reactor condensed tars and water from the volatiles. Permanent gases were sampled near the cold trap exit at preselected times during the experiment using two automated gas sampling valves, thus providing information on evolution rates of gaseous products. All volatiles were later analyzed by gas chromatography.

**Sample Preparation** - The wood pellets were all cut, with great attention to grain direction, from uniform sections of the same lodge pole pine tree provided by Weyerhaeuser Co. (Corvallis Mill). The cylinders were oven-dried at  $90 \text{ C}$  for at least three weeks. Moisture was quantitatively added using a microsyringe and balance, and allowed to come to a uniform distribution as described by Kelbon (13).

**Gas Analysis** - Permanent gases, operationally defined as all components passing through the  $-40 \text{ C}$  cold trap, were collected in 30 stainless steel sample loops of known volume. Immediately after the experiment, samples were automatically injected into a Perkin-Elmer Sigma 2 Gas Chromatograph using a Supelco 100/120 mesh Carbosieve S column  $1/8 \text{ in.}$  diameter and 5 ft. long. The peaks were integrated and identified by a Perkin-Elmer Sigma 15 Chromatography Data Station. Both a thermal conductivity detector and a flame ionization detector were used as described in Bousman (14).

**Tar Analysis** - The tar is comprised of two parts, that which was trapped and that which was washed from the reactor, though the latter is often a small amount. The tar trap sample was analyzed for water and low molecular weight tar compounds by gas chromatography using a Supelco 80/100 mesh Porapak Q column  $1/8 \text{ in.}$  diameter and 1.5 ft long. After the low molecular weight tar analysis, the trap tar and reactor tar samples were treated with approximately 2 g of  $\text{MgSO}_4$  to remove water and then filtered. A known quantity of p-bromophenol was added to each sample as an internal standard. Each sample was concentrated in order to remove THF while minimizing the loss of the other compounds. The resulting high molecular weight tar liquid was analyzed by gas chromatography using either a J and W Scientific DBWAX or Carbowax 20M fused silica capillary column  $0.25 \text{ mm ID, 30 m}$  long with a Perkin-Elmer splitting injection port. The major peaks which appeared in the

majority of the samples are numbered and presented in this paper as simplified, composite chromatograms.

**Char Analysis** - The char was weighed and a qualitative chemical analysis of some char samples was performed using a Fourier Transform Infrared Spectrometer (FTIRS) with preparation as described in Bousman (14). The surface area of the char was also characterized using CO<sub>2</sub> adsorption.

**Experimental Design** - The experimental conditions were picked according to a type of factorial experimental design which facilitates identification of optima and empirical models of the class given in Eq. 1 (11,15):

$$y_k = b_0 + \sum b_i x_i + \sum \sum b_{ij} x_i x_j, \quad \text{for } i \leq j, \quad (1)$$

where

$y_k$  is the k-th product yield of interest,

$x_i, x_j$  are the independent variables (process controllables) and

$b_0, b_i$  and  $b_{ij}$  are least square parameter estimates obtained from multiple regression.

When variables combine to affect the reaction process in a non-additive way, as when the last term of Eq. 1 is large, non-linear dependence of yields on the process controllables is demonstrated. Plots of Eq. 1 are presented in subsequent figures as trend lines.

## RESULTS AND DISCUSSION

The range of intraparticle temperatures measured throughout pyrolysis at a constant heat flux of 4 cal/cm<sup>2</sup>-s for a particle initially at 60% moisture (Fig. 1) corresponds to those found in other studies for both small (16-18) and large (19) particles. As can be seen when moisture is added, the temperature rises in the first ~30 sec to a plateau at 100 C until the water has locally evaporated, and then the temperature rises to the same level as found in dry wood particles, although at a somewhat later time. The surface temperature is of some qualitative value but once volatiles are produced, the infrared pyrometer cannot accurately "see" the surface and the measured temperature is artificially low. Note that reaction in zones near the surface experience quite high heating rates, which should favor tar production early in the devolatilization of a large particle.

In this preprint, overall yields are reported as graphs rather than tables, and correspond to time-integrated pyrolysis or devolatilization products from a large wood particle heated under constant applied heat flux at the surface. The yields are expressed as weight fractions of that which reacted in the 12 min pyrolysis duration. Fractional yields are an important measure of selectivity and are useful for downstream separation process considerations. The appropriate measure of experimental reproducibility and accuracy is the standard error calculated from replicate runs. This is given as an uncertainty. However, because of the inherent difficulty in recovering all products, especially tars, the mass balances do not always add to 100%. Thus, another measure of error is the discrepancy in the mass balance. For these experiments, the average mass balance closure was 80%, with a standard deviation of 11%.

In Fig. 2 the weight fraction water-free tar produced from the fixed duration pyrolysis of dry wood particles of several thicknesses is presented. The symbols, when there are two at the same heat flux, represent tar yield for 2 different particle densities. It can be seen that a 0.3 g/cc density change has little effect on tar yield. The trend lines result from regression of all the data to a single set of parameters for Eq. 1. The average prediction error as approximated by the standard error of the residuals is 2%, and the standard deviation of replicate runs is the same. In Fig. 2, the synergy, or interaction of particle size and heat flux can be clearly seen. The reduction in tar for an increase in heating rate, as characterized by the slope of the trend lines at any point, increases as the particle thickness increases. The thickest particle pyrolyzed at the lowest heat flux produces over 65% tar, and it decreases to 20% at the maximum intensity investigated. This is consistent with the extensive tar cracking that likely occurs near the particle surface char zone where high temperatures prevail

for severe heating. Note that all dry particles heated at the intermediate heat flux result in approximately 25%-35% tar.

The pyrolytic tar produced from a wet wood particle is presented in Fig. 3 as a function of both initial moisture content (abscissa) and heating intensity for the thickest particle size used in this study, 1.5 cm. The prediction error and the experimental error in the measured tar from wet particle pyrolysis is about 5%. Note that moisture causes the optimum tar conditions to occur at 4 cal/cm<sup>2</sup>-s, rather than the 2 cal/cm<sup>2</sup>-s for dry particles, consistent with the lower particle temperature expected when water is present. Overall, the level of tar produced is considerably higher, 50-70%, than for dry wood particles. Hydrogen is measured in the gases, as well.

In Fig. 4, a composition profile of some components of both tar and gas is presented. Changes in this profile simply highlight changes in composition as process conditions change. The ordinate is the weight fraction of the reacted portion of the 1 cm particle data used in this figure. Thus all components plotted are each less than 2% of the moist wood particle that was pyrolyzed. The error as estimated from replicated determinations is about 0.5%. The high molecular weight species composition appears to vary little as particle temperature is manipulated by changing both moisture and heating intensity of the pyrolysis. However, the low molecular weight tar compounds are in greater concentration for mild intensity heating (2 cal/cm<sup>2</sup>-s) than for a greater heating rate which appears to favor the hydrocarbon gases and hydrogen. Although the composition differences are nearly within the experimental error, moisture appears to slightly enhance the production of methanol and acetic acid for these experiments (1 cm particle).

## CONCLUSIONS

Data has been presented which suggests that moisture can enhance the production of tar from the pyrolysis of large wood particles using conditions that occur in a large scale reactor where the heat flux a particle experiences is quite constant. The most favorable conditions result in about 70% of the reacted biomass becoming tar. If one assumes that the mass balance discrepancy results from tar condensing on reactor surfaces, this is a conservative estimate.

## ACKNOWLEDGEMENTS

This work was supported by the National Science Foundation, Grant No. CPE- 8400655. Marcia Kelbon gratefully acknowledges the support of a Weyerhaeuser Fellowship and Scott Bousman acknowledges the fellowship support of Chevron Corp.

## REFERENCES

1. Cady, T., personal communication, Weyerhaeuser Corp., Cosmopolis, WA, 1982.
2. Petersen, E.E., *Chemical Reaction Analysis*, Prentice Hall, 1965.
3. Russel, W.A., D.A. Saville, and M.I. Greene, *AIChEJ.* 25, 65 (1979).
4. Srinivas, B. and N.R. Amundson, *AIChE J* 26, 487 (1980).
5. Massaquoi, J.G.M., and J.B. Riggs, *AIChEJ* 29, 975 (1983).
6. Chan, W.C.R., Ph.D. Thesis, Dept. Chem. Engrg., U. Washington, 1983.
7. Lee, C.K., R.F. Chaiken, and J.M. Singer, *16th International Symposium on Combustion*, Combustion Institute, Pittsburgh, PA, 1459 (1976).
8. Ohlemiller, T. K. Kashiwagi, and K. Werner, NBSIR 85-3127, NBS Center for Fire Research, April 1985.
9. Miles, T.R., *Thermochemical Processing of Biomass*, Ed. by A.V. Bridgewater, Butterworths, London, p. 69 (1984).
10. Chan, W.C.R., submitted to *I.E.C. Proc. Des. Dev.*, (1986).
11. Box, G.E.P. and D.W. Behnken, *Technometrics* 2, 455 (1960).
12. Chan, W.C.R., M. Kelbon, B.B. Krieger, *Fuel* 64 1505(1985).
13. Kelbon, M., M.S. Thesis, Dept. Chem. Engrg., U. Washington, 1983.
14. Bousman, W.S., M.S. Thesis, Dept. Chem. Engrg., U. Washington, 1986.
15. Box, G.E.P., J.S. Hunter, W.G. Hunter, *Statistics for Experimenters*, Wiley, 1978.

16. Scott, D.S., J. Piskorz, and D. Radlein, *I.E.C. Proc. Des. Dev.* 24 , 581 (1985).
17. Nunn, T.R. J.B. Howard, J.P. Longwell, and W.A. Peters, *I.E.C. Proc. Des. Dev.* 24 , 836 (1985).
18. Bradbury, A.G.W. F. Sakai, and F. Shafizadeh, *J. Appl. Poly. Sci.* 23, 3271 (1979)
19. Kanury, A.M., *Combustion and Flame* 18 , 75 (1972).

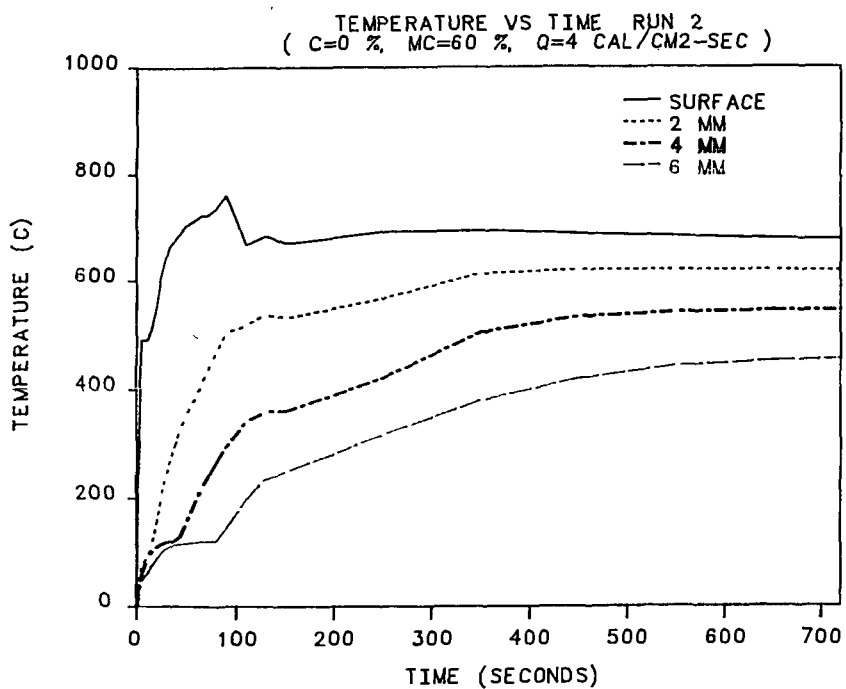


Fig. 1 - Temperature histories at 4 positions in a 1 cm thick wood particle pyrolyzed with an applied heat flux of 4 cal/cm<sup>2</sup>-s.

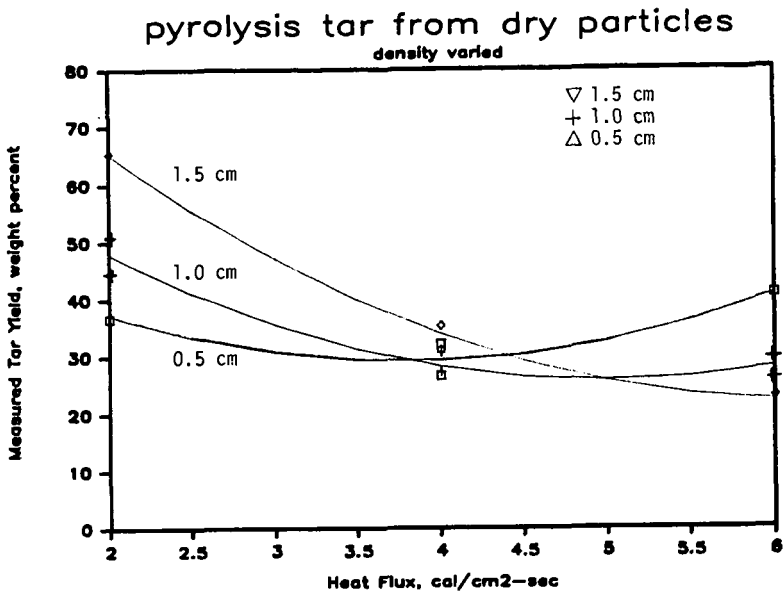


Fig. 2 - Weight fraction tar yield for the pyrolysis of dry wood particles at varying surface heat fluxes for three thicknesses; trend lines are least square fits and symbols are some of the experimental data.

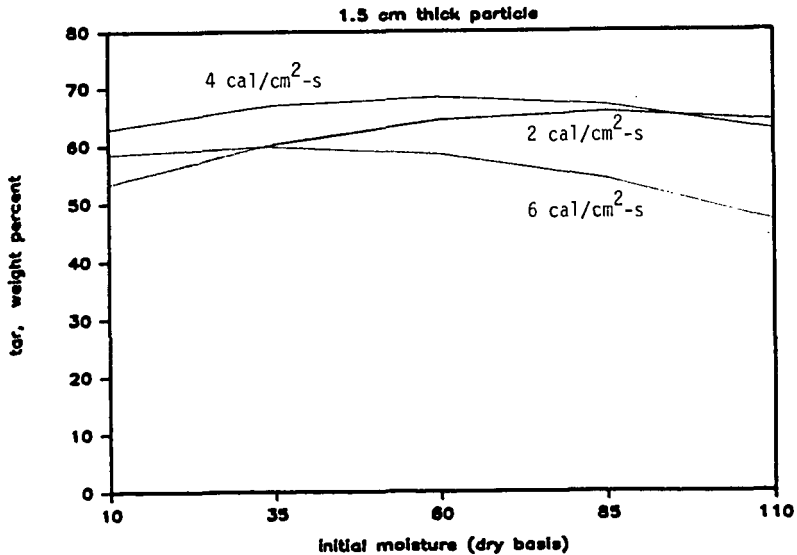
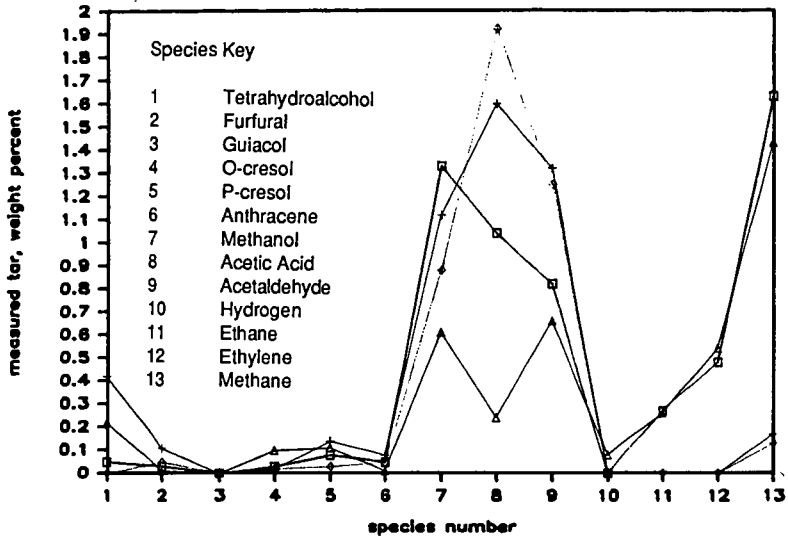


Fig. 3 - Measured weight fraction tar produced from a 1.5 cm thick wood particle as a function of moisture content for 3 different heating rates.

## pyrolysis product profile



### Symbol Key

- + 110% initial moisture, heated at 2 cal/cm<sup>2</sup>-s
- ◇ 10% initial moisture, heated at 2 cal/cm<sup>2</sup>-s
- 110% initial moisture, heated at 6 cal/cm<sup>2</sup>-s
- △ 10% initial moisture, heated at 6 cal/cm<sup>2</sup>-s

Fig. 4 - Product composition profile for two moisture content 1 cm thick particles heated at two heating rates.

## Effects of Extra-particle Secondary Reactions of Fresh Tars on Liquids Yields in Hardwood Pyrolysis

Michael L. Boroson, Jack B. Howard, John P. Longwell,  
and William A. Peters

Department of Chemical Engineering and Energy Laboratory  
Massachusetts Institute of Technology  
Cambridge, MA 02139

### Introduction

Wood pyrolysis involves a complex system of chemical and physical processes. It is not yet possible to identify and model the individual reactions occurring during pyrolysis; however, a simplified model using lumped product groups such as tar, char, and gases can provide insight into the overall process.

Upon heating wood decomposes by an unknown series of bond-breaking reactions. The species formed by this initial step may be sufficiently immobile to preclude rapid escape from the particle. Consequently they may undergo additional bond-breaking reactions to form volatiles or may experience condensation/polymerization reactions to form higher molecular weight products including char. During transport within the particle volatile species may undergo further reactions homogeneously in the gas phase or heterogeneously by reaction with the solid biomass or char. The rate of volatiles mass transport within and away from the particle will influence the extent of these intraparticle secondary reactions. After escaping the particle, the tars and other volatiles may still undergo secondary reactions homogeneously in the vapor phase or heterogeneously on the surface of other biomass or char particles. Depending on reaction conditions intra- and/or extra-particle secondary reactions can exert modest, to virtually controlling influence on product yields and distributions from wood pyrolysis.

There exists a substantial amount of literature on the primary pyrolysis of wood. The literature on homogeneous secondary reaction kinetics of wood pyrolysis tars, however, is limited to only two studies (1,2) and no literature exists on the heterogeneous secondary reactions of tar over fresh wood char. The objective of the present study, therefore, was to obtain improved quantitative understanding of the homogeneous and heterogeneous extra-particle secondary reactions of sweet gum hardwood pyrolysis tar under conditions pertinent to gasification, combustion, and waste incineration. Sweet gum hardwood was chosen for two reasons: (a) this type of wood has commanded interest as an energy crop in the southern United States, and (b) secondary reaction results can be compared to sweet gum hardwood primary pyrolysis results already reported in the literature (3).

Results on homogeneous tar cracking are presented below. Studies of heterogeneous cracking of tar vapors over freshly generated wood char are in progress. Results will be presented.

### 1. Experimental

Yields of individual primary and secondary pyrolysis products as affected by reaction conditions and physical and chemical characteristics of "primary" (newly formed) and "secondary" (surviving thermal treatment) tar samples, were needed to fulfill the study objectives.

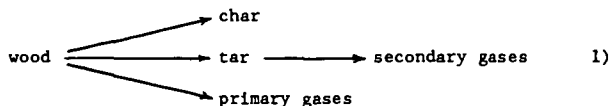
A two-chamber tubular reactor (Fig. 1) developed by Serio (4) for systematic studies of secondary reactions in coal pyrolysis, was adapted for the present measurements. In this apparatus "primary" tar, *i.e.*, tar that has undergone minimal extra-particle secondary reactions, is generated in an upstream reactor (No. 1) by heating a shallow packed bed of biomass, usually at a constant heating rate (typically 12°C/min). This tar and other volatiles are rapidly swept into a second reactor (No. 2) by a continuous flow of carrier gas (helium with an argon tracer). Here the volatiles are subjected to controlled extents of post-pyrolysis thermal treatment at temperatures between 400 to 800°C, pressures from 120 to 250 kPa, homogeneous residence times (V/F) between 0.9 and 2.2 sec, and heterogeneous space times ( $V_b/F$ ) between 5 and 200 msec.

Four reactor configurations have been employed in the present investigation. In Mode I runs, only the first-stage reactor is used, and freshly evolved wood pyrolysis products spend little time at high reaction severities. Thus they reflect minimal contributions from secondary reactions and are taken as well representative of the tars evolved near the wood surface. In the present work tars so evolved will be defined as "primary" tars. In Mode II runs, only the second-stage reactor is used, and yields and surface characteristics of fresh char as a function of initial wood bed depth are determined. In Mode III runs, the empty second reactor is connected downstream of Reactor 1, preheated, and then maintained isothermal. Homogeneous secondary reactions of wood tar vapors are studied quantitatively by controlling their extent of thermal treatment in this reactor and measuring its effect on product yields, tar loss and tar composition. In Mode IV runs, the second reactor is packed with a mixture of wood and quartz and again connected downstream of Reactor 1. Reactor 2 is first heated to 800°C to generate the fresh char then cooled to the desired reaction temperature prior to heating Reactor 1. Heterogeneous secondary reactions of wood tar vapors are studied by varying the temperature and heterogeneous residence time over the bed of char and quartz.

Product characterization includes quantifying tar and light volatiles yields, and global analysis of tars. A Perkin-Elmer Sigma 2B Gas Chromatograph was used to determine the yields of carbon monoxide, carbon dioxide, methane, acetylene, ethylene, ethane, and C<sub>3</sub> hydrocarbon gases. Size exclusion chromatography (SEC) was used to determine the weight averaged molecular weights of the primary and secondary tars. The equipment is a Waters Associates ALC/GPC 201 SEC system with two  $\mu$ styragel columns, 500 and 100 Å, in series, and a 405 nm UV detector.

## 2. Mathematical Modeling

Wood pyrolysis involves a complex set of parallel and series chemical reactions frequently influenced by heat and mass transfer, and tractable models generally must be built upon simplifying assumptions. Our model assumes the following reaction sequence:



and describes each of the above pathways with a single-reaction, first-order rate constant, the parameters for which are determined by curve-fitting product yield data. The kinetic parameters for the formation of char, tar, and primary gases from pyrolysis of the same sweet gum hardwood used in this study have been reported (3). The present modeling focuses on homogeneous cracking of the tar vapor and on the secondary gas formation reactions.

Net cumulative yields of unreacted tar and of individual gaseous products from tar vapor cracking were calculated as the difference between the cumulative amount of each entering (from Mode I runs) and leaving (from Mode III runs) Reactor 2. The data were then fit to the kinetic equation

$$\frac{dV_i}{dt} = k_i(V_i^* - V_i) \quad 2)$$

where  $V_i$  is the yield of material  $i$  at time  $t$ ,  $V_i^*$  is the ultimate value of  $V_i$  at long residence times and high temperatures, and  $k_i$  is the global rate coefficient. Thus the rate of tar cracking at any time is modeled as first order in the difference between the ultimate (minimum) yield of tar (wt% of nonreactive tar) and the total amount of tar unconverted at that time. The rate of formation of an individual gaseous product is first order in the difference between the ultimate (maximum) yield of that gas and the amount of that gas generated up to that time. The kinetic parameters for homogeneous tar cracking and individual gaseous product

formation were found by a least squares parameter fitting technique.

### 3. Results and Discussion

Approximately fifty runs were performed to generate a broad data base on product yields as a function of primary and secondary reactor operating parameters. Good overall material balances and reproducibility were obtained. Selected tars collected from these runs were further characterized by SEC.

#### 3.1 Homogeneous Cracking Product Yields

Product yields were determined for each experiment as described in Section

1.2. Representative yields for primary pyrolysis of wood and for homogeneous secondary tar cracking at 600, 700, and 800°C are shown in Table 1.

Primary pyrolysis products from the first reactor were tar, char, water, carbon dioxide, carbon monoxide, and a trace of methane. More reactive primary products, such as tar, become reactants for secondary reactions, when the thermal treatment reactor (Mode-III) is in place. These secondary reactants, and products arising from their secondary reactions can in turn be identified by observing whether their yield increases, decreases, or remains constant when changing from Mode I to Mode III, or when increasing the Mode III temperature. Tar, for example, is a primary product and a secondary reactant as demonstrated by its high yield from Mode I experiments and its decreasing yield with increasing reaction severity in Mode III experiments. For residence times of about 1 sec. homogeneous tar conversion ranged from 9wt% at 500°C to 30wt% at 600°C and up to 88wt% at 800°C.

Carbon dioxide is both a primary and secondary product, since the yield in Mode I is about half the total CO<sub>2</sub> yield from high severity Mode III runs (800°C, Table 1). Carbon dioxide accounted for about 14% of the tar lost during secondary tar cracking.

Carbon monoxide and methane are evolved in modest quantities from Reactor 1. However, most of the production of these compounds along with acetylene, ethylene, ethane, and hydrogen arises from secondary reactions as evidenced by their substantial yield increases in the Mode-III experiments.

Carbon monoxide was the major product of secondary tar cracking at all temperatures, accounting for about 60-70wt% of the tar cracked. Methane and ethylene accounted for about 10 and 11wt% of the tar cracked, respectively, and the remaining 2-4wt% of the tar was cracked to form acetylene, ethane, and hydrogen. At high tar cracking severities (> 85%) the dry gas composition by volume was 48% CO, 19% H<sub>2</sub>, 13% CH<sub>4</sub>, 11% CO<sub>2</sub>, and 7% C<sub>2</sub>H<sub>4</sub>, with traces of C<sub>2</sub>H<sub>2</sub> and C<sub>2</sub>H<sub>6</sub>.

Negligible amounts of char were observed in the second stage of the tubular reactor upon completion of experiments on homogeneous cracking of tar vapor. This implies that when char formation is observed in wood pyrolysis other pathways such as liquid phase tar condensation reactions, possibly surface assisted, are responsible. This picture is consistent with the ablative pyrolysis studies of Lede et al. (5) who found that char formation in wood devolatilization can be prevented by rapidly removing prompt pyrolysis tar liquids from wood surfaces at elevated temperature.

#### 3.2 Tar characterization

The tar samples collected after different extents of homogeneous secondary thermal treatment were characterized by size exclusion chromatography (SEC). The weight average molecular weight behavior of tars as a function of conversion is shown in Figure 1. As shown, the average molecular weight of tar surviving secondary cracking is lower than the molecular weight of primary tar (640 gm/mole) entering the cracking reactor. Average molecular weights tend to decrease with increasing conversion; however, the change in average molecular weight over the range of conversion 20-80% is small after a sharp drop in average molecular weight from zero to ten percent conversion. This behavior is consistent with tar cracking occurring by a random scission mechanism.

#### 3.3 Homogeneous Kinetics

Yield data from the tubular packed bed reactor were used to calculate kinetic

parameters as described in Section 2. Resulting best fit kinetic parameters for formation of secondary gases and for the homogeneous cracking of tar are given in Table 2.

The extent of secondary reaction is a function of both temperature and time. The separate effects of temperature and time can be described by a single parameter called "reactor severity," equal to the product of the rate constant at the reactor temperature and the isothermal residence time. Plots of the experimental yield of tar and individual gaseous products as a function of the dimensionless reactor severity ( $kt$ ) are shown in Figures 2 - 5 together with smooth curves denoting the corresponding model predictions. The model predicts the experimental yields with an error generally less than ten percent.

Homogeneous kinetic results of this study were compared to results found in the literature. Vapor phase cracking of wood pyrolysis tars from an unspecified softwood was studied by Diebold (1) and cracking of tars from both cherry and yellow pine was studied by Mattocks (2). Due to differences in product group definitions as well as modeling techniques and assumptions, our results could not be directly compared to the results of Mattocks.

Diebold's kinetic parameters for the cracking of volatiles to gases ( $A = 10^{5.19} \text{ sec}^{-1}$ ,  $E = 87.5 \text{ kJ/mole}$ ) are comparable to the tar cracking parameters from this study ( $A = 10^{4.98} \text{ sec}^{-1}$ ,  $E = 93.3 \text{ kJ/mole}$ ). Over the common temperature range of experimentation (650 - 800°C) the rate constant of Diebold is only 3 - 3.5 times higher than that found in this work despite the differences in the reactor type and wood producing the primary volatiles. The small discrepancy could be due to effects of wood type, to slight differences in the models, or to Diebold's need to calculate the gas composition entering the isothermal section of his volatiles cracking reactor. In the present work the entering gas composition is measured directly in the Mode I runs.

#### 4. Conclusions and Significance

The experimental results of this study identified and quantified those products generated by primary pyrolysis of wood and those formed by extra-particle secondary cracking of newly-formed wood pyrolysis tar. Tar, char, water, and carbon dioxide are primary products of wood pyrolysis. Additional carbon dioxide, however, is also formed by vapor phase cracking of tar. Carbon monoxide, hydrogen, methane, ethylene, acetylene, and ethane are products of homogeneous secondary cracking of wood tars, although modest amounts of CO, and trace quantities of methane are also observed under conditions chosen to arrest vapor phase tar cracking (Mode I). Carbon monoxide accounts for about 65 wt% of the products when fresh wood tar undergoes vapor phase cracking.

Tars surviving various extents of post pyrolysis secondary thermal cracking were characterized by size exclusion chromatography (SEC). SEC indicates that tars surviving vapor phase cracking are lower in weight-average molecular weight than the uncracked tars. In addition, there was no evidence for tar molecular weight growth among these surviving tars. This result is consistent with the experimental observation of negligible coke production during vapor phase tar cracking.

The experimental yields of the individual gaseous products from homogeneous cracking of wood pyrolysis tar can generally be predicted by global single-reaction first-order kinetic models to within better than ten percent. These first-order kinetic parameters are sufficiently intrinsic to be used in reactor design calculations including predictions of the contributions of extra-particle homogeneous vapor phase tar reactions. These parameters can also be used to estimate the kinetics of intra-particle homogeneous reactions of tar vapor, but further work will be needed to define the validity of this application.

#### Notation

- $A_1$  - Arrhenius pre-exponential factor for species 1
- $E_1$  - apparent Arrhenius activation energy for species 1
- $k_1 = A_1 \exp(-E_1/RT)$  - Arrhenius rate constant
- R - gas constant
- T - absolute temperature

$V_1^*$  - ultimate yield in weight percent of wood of species 1  
 $V_1$  - yield in weight percent of wood of species 1  
 $V$  - volume of reactor 2  
 $V_b$  - volume of char bed in reactor 2  
 $F$  - volumetric gas flow rate at reactor 2 temperature

#### Acknowledgements

Most of the above work was supported by the National Science Foundation, Division of Chemical and Process Engineering, Renewable Materials Engineering Program, under Grant Nos. CPE-8212308 and CBT-8503664. We also gratefully acknowledge an NSF Fellowship for M. Boroson and financial support by the Edith C. Blum Foundation of New York, NY and the Robert C. Wheeler Foundation of Palo Alto, CA. Drs. M. K. Burka, J. Hsu, L. Mayfield, and O. R. Zaborsky (NSF) have served as technical project officers. Christine Clement and Anne Reeves have made valuable contributions to this work.

#### Literature Cited

1. Diebold, J. P., "The Cracking Kinetics of Depolymerized Biomass Vapors in a Continuous, Tubular Reactor," M.S. Thesis, Dept. of Chemical and Petroleum-Refining Engineering, Colorado School of Mines, Golden, Colorado (1985).
2. Mattocks, T. W., "Solid and Gas Phase Phenomena in the Pyrolytic Gssification of Wood," M.S. Thesis, Dept. of Mechanical and Aerospace Engineering, Princeton University, Princeton, New Jersey (1981).
3. Nunn, T. R., J. B. Howard, J. P. Longwell, and W. A. Peters, "Product Compositions and Kinetics in the Rapid Pyrolysis of Sweet Gum Hardwood," Ind. Eng. Chem. Process Design Develop., 24, 836-844, (1985).
4. Serio, M. A., "Secondary Reactions of Tar in Coal Pyrolysis," Ph.D. Thesis, Dept. of Chemical Engineering, MIT, Cambridge, Massachusetts (1984).
5. Lede, J., J. Panagopoulos, and J. Villermaux, "Experimental Measurement of Ablation Rate of Wood Pieces, Undergoing Fast Pyrolysis by Contact With a Heated Wall," Am. Chem. Soc. Div. of Fuel Chem. Preprints, 28 (5), 383 (1983).

Table 1. Product Yields (weight % of wood)  
 as a Function of Thermal Treatment

	Primary Yields	Secondary Reaction Yields		
		600°C 1.2 s	700°C 1.0 s	800°C 1.0 s
Tar	52.8	36.6	16.6	6.1
Char	18.3	18.1	18.4	17.8
CH <sub>4</sub>	0.4	1.7	3.8	5.5
CO	3.2	14.7	25.7	35.7
CO <sub>2</sub>	6.8	9.7	11.4	13.2
C <sub>2</sub> H <sub>2</sub>	0.0	0.1	0.5	0.6
C <sub>2</sub> H <sub>4</sub>	0.0	1.2	3.6	5.4
C <sub>2</sub> H <sub>6</sub>	0.0	0.1	0.3	0.4
H <sub>2</sub> O	16.3	17.3	17.0	15.2
H <sub>2</sub>	0.0	0.1	0.6	1.0

Table 2: Kinetics Parameters for Gas Formation and Tar Cracking

	log A (sec <sup>-1</sup> )	E (kJ/mole)	v* (wt% of wood)
CH <sub>4</sub>	4.89	94.1	5.83
C <sub>2</sub> H <sub>4</sub>	5.76	109.3	5.17
C <sub>2</sub> H <sub>6</sub>	7.52	138.8	0.38
CO <sub>2</sub>	2.55	48.8	13.20
CO	4.66	87.8	36.33
H <sub>2</sub>	6.64	128.4	1.09
TAR	4.98	93.3	5.79

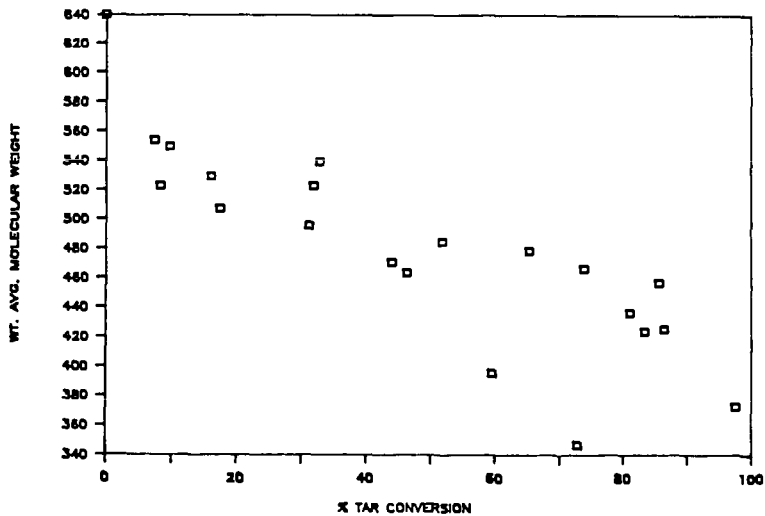


Figure 1: Effect of Vapor Phase Thermal Treatment on Weight Average Molecular Weight of Surviving Tar

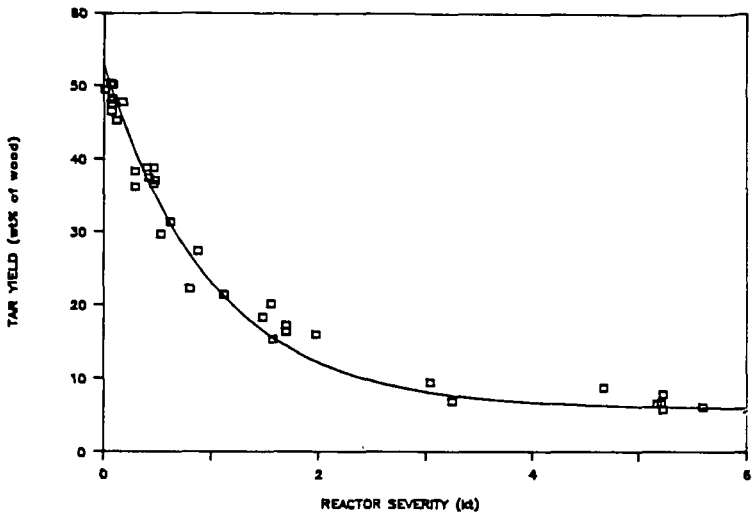


Figure 2: Effect of Reactor Severity on Tar Yield (— model prediction)

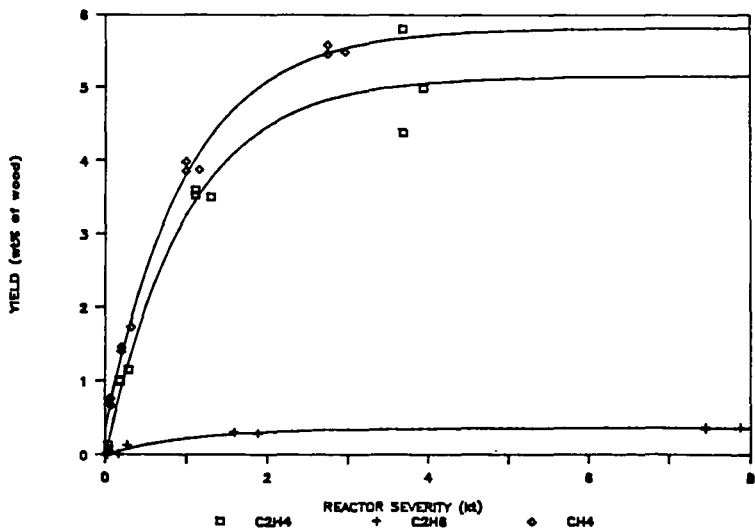


Figure 3: Effect of Reactor Severity on Ethylene, Ethane, and Methane Yields (— model prediction)

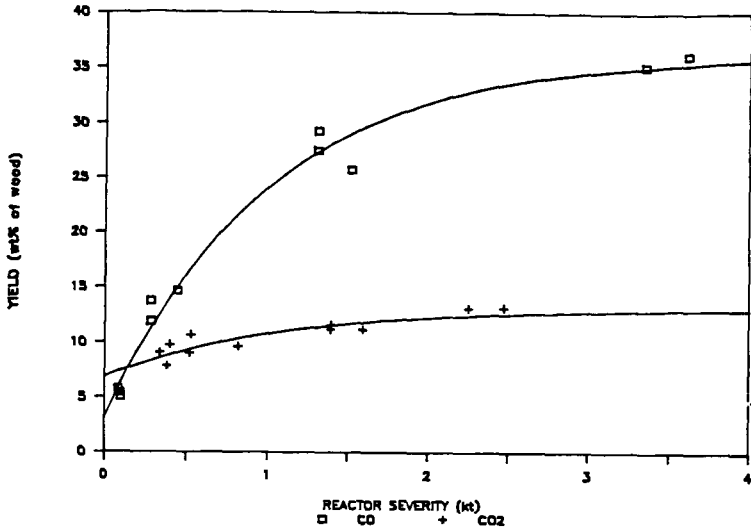


Figure 4: Effect of Reactor Severity on Carbon Monoxide and Carbon Dioxide Yields ( — model prediction)

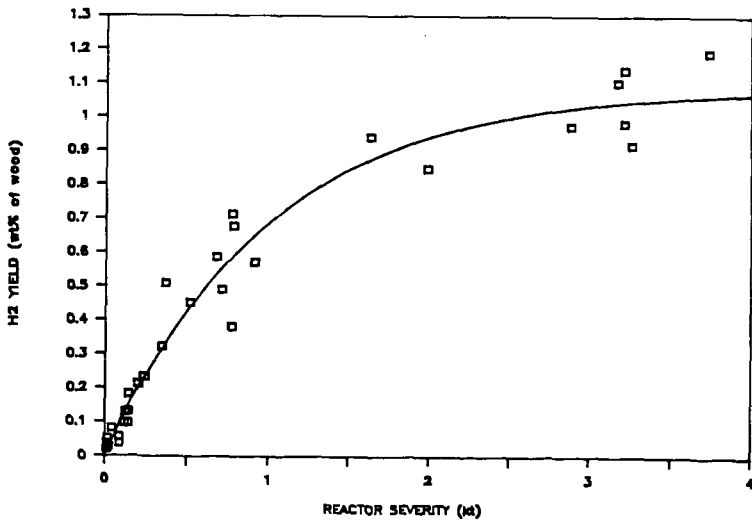


Figure 5: Effect of Reactor Severity on Hydrogen Yield ( — model prediction)

## FUSION-LIKE BEHAVIOUR OF BIOMASS PYROLYSIS

Jacques LEDE, Huai Zhi LI and Jacques VILLERMAUX

Laboratoire des Sciences du Génie Chimique, CNRS-ENSIC  
1, rue Grandville 54042 NANCY (FRANCE)

### INTRODUCTION

Considering a thermal reaction of a Solid  $\rightarrow$  Fluid type, the apparent rate of reaction can be controlled by chemistry, thermal and mass transfer resistances. If the chemical processes are very fast, and if the fluid products are easily eliminated from the medium, the overall rate of reaction is controlled by heat transfer resistances. This is the case of the ablation regime [1], characterized by a steep temperature gradient at the wood surface and consequently by a thin superficial layer  $e$  of reacting solid moving at a constant velocity  $v$  towards the cold unreacted parts of the solid.

Suppose now that heat is provided by a surface at  $T_W$ . A theoretical increase of the surface temperature  $T_D$  of the solid (by increasing  $T_W$ ) would lead to a subsequent increase of the heat flux demand. Such a demand would be satisfied by an equal external heat flux supply, a condition fulfilled only with large temperature gradients ( $T_W - T_D$ ). The consequence would be a stagnation of  $T_D$ , leading to a fusion like behaviour of the reaction.

Wood pyrolysis carried out in conditions of high available heat fluxes and efficient elimination of products occurs in ablation regime with production of very low fractions of char [2,3,4] and could therefore behave as a simple fusion. This paper presents a brief outline of the main ideas and results obtained to this effect and issued from different approaches. More details can be found in related papers [5,6,7,8].

The reaction has been carried out in three different conditions : heating against a hot spinning disk ; against a fixed heated surface ; in a continuous cyclone reactor. In the first two cases, the behaviour of the reaction is compared to that of solids undergoing simple fusion in the same conditions.

### SPINNING DISK EXPERIMENTS

The melting of ice, paraffin and "rilsan" (polyamide 11) and the pyrolysis of wood have been carried out by applying under known pressures  $p$ , rods of the corresponding solids against a hot spinning stainless steel disk (temperature  $T_W$ ) [5,6]. In wood experiments, the reaction produces almost exclusively gases and liquids, the solids being mainly ashes deposited on the disk. The liquids produced are rapidly extracted from the wood surface and eliminated by the fast moving disk on which they undergo further decomposition to gases at a rate depending on  $T_W$ . The presence of the thin liquid layer acts as a kind of lubricant.

Figure 1 reveals that under comparable values of  $p$ , the behaviour of  $v$  as a function of  $v_R$  is similar, the orders of magnitude of  $v$  being the same for the four types of solids. For  $v > 2 \text{ m s}^{-1}$ ,  $v$  increases with  $p$  following :

$$v = a p^F$$

(1)

a depends on  $T_w$  and F on the material. The mean values of F (ice : 0.035 ; paraffin : 0.29 ; "rilisan" : 0.83 ; wood : 1) can be fairly well represented by :

$$F(\text{melting solid}) = \frac{Cp_s(T_f - T_o)}{Cp_s(T_f - T_o) + L} \quad \text{or} \quad F(\text{wood}) = \frac{Cp_s(T_d - T_o)}{Cp_s(T_d - T_o) + \Delta H} \quad (2)$$

F being close to 1 for wood shows that it is probable that  $\Delta H$ , the enthalpy of pyrolysis, is small with respect to sensible heat in agreement with literature.

The equations of heat flux density balances between the disk and the rod are :

$$\begin{aligned} \text{melting solid} : h(T_w - T_f) &= v\rho_s Cp_s (T_f - T_o) + v\rho_s L \\ \text{wood} : h(T_w - T_d) &= v\rho_s Cp_s (T_d - T_o) + v\rho_s \Delta H \end{aligned} \quad (3)$$

Assuming that the heat transfer coefficient h is the only parameter depending on the pressure ( $h = Kp^F$ ) it can be deduced :

$$\frac{v}{p^F} (\text{melting solid}) = \frac{K}{\rho_s Cp_s (T_f - T_o) + L} \frac{T_w - T_f}{p^F} ; \quad \frac{v}{p^F} (\text{wood}) = \frac{K}{\rho_s Cp_s (T_d - T_o) + \Delta H} \frac{T_w - T_d}{p^F} \quad (4)$$

In agreement with (4), Figure 2 shows that the variations of  $\frac{v}{p^F}$  with  $T_w$  are linear for the three melting solids and also for wood. The values of  $T_f$  calculated from the extrapolation of the straight lines to  $v = 0$  are in very good agreement with the known values of melting points (better than 2 % accuracy). The corresponding "fusion temperature" of wood is then calculated close to 739 K.

The values of heat transfer coefficients obtained from the slopes of the straight lines in figure 2 are of the same order of magnitude (around  $10^4 \text{ W m}^{-2} \text{ K}^{-1}$ ) whatever the solid showing that the mechanisms of heat transfer are probably similar for wood and melting solids. For wood, h varies as  $h = 0.017 p (\text{W m}^{-2} \text{ K}^{-1}) [5]$ . These values reveal very efficient transfers.

#### FIXED HEATED WALL

The same experiments as before have been made with rods of ice, paraffin and wood pressed against a stationary piece of brass heated at  $T_w$ .

An analytic solution has been found for representing the rate of ablative melting of a solid cylinder pressed against a horizontal wall maintained at  $T_w$  [7]. In steady state, a liquid layer of constant thickness is formed between the hot surface and the rod, with a radial flow of liquid. The resolution of the equation of liquid flow associated with that of energy balance between the two surfaces allows to derive the following relationship:

$$v = \frac{\rho_l}{\rho_s} \left[ \frac{2}{3} \frac{\alpha_l^3}{\mu_l R^2} Pe^3 (Ph) p \right]^{1/4} \quad (5)$$

where Pe is a Peclet number, a function of a phase change number

$$Ph = \frac{Cp_l (T_w - T_f)}{L} \quad \text{as} \quad Pe = \frac{Ph}{1 + Ph^{5/6}/3}$$

The relation (5) shows that v varies as  $p^{0.25}$  whatever the type of solid. In reduced form, (5) can be written as follows :

$$v = \frac{2}{3} [Pe^3 P]^{1/4} \quad (6)$$

with 
$$v = \frac{\rho_s R}{\rho_l \alpha_l} v \quad \text{and} \quad P = \frac{R^2}{\mu_l \alpha_l} p$$

By plotting  $V$  against  $\left[\frac{2}{3} Pe^3 P\right]^{1/4}$  one should obtain a straight line of slope one whatever the nature of melting solid and wall temperature.

As in the case of ice and paraffin [7], ablation rate  $v$  for wood pyrolysis varies as  $P^F$  with a mean value of  $F$  (0.29) close to the theoretical one (0.25) (Fig. 3). The figure 4 gathers all the experimental points according to (7). The physical properties used for the calculation of  $V$  and  $P$  for ice and paraffin are reported in ref. [7,8]. In the case of wood, the factor containing these properties in equation (5) has been fitted to the experimental results (fig. 3) leading to  $v = 1.55 \times 10^{-3} (Pe^3 p/p_0)^{1/4} (m s^{-1})$ . The fitted constant associated with estimated values for  $\rho_l$  ( $500 \text{ kg m}^{-3}$ ),  $Cp_l$  ( $3.65 \text{ kJ.kg}^{-1}\text{K}^{-1}$ ) and  $\alpha_l$  ( $0.3 \times 10^{-7} \text{ m}^2 \text{ s}^{-1}$ ) allows to calculate  $\mu_l = 72.5 \times 10^{-3} \text{ Pa.s}$ , a reasonable value for the viscosity of a liquid at a melting point of 739 K [7,8].

#### CYCLONE REACTOR EXPERIMENTS

The continuous fast pyrolysis of wood sawdust has been studied in a Lapple type ( $2.8 \times 10^{-2} \text{ m}$  diameter) cyclone reactor heated between 893 and 1330 K [2]. The wood particles carried away by a flow of steam enter tangentially into the cyclone on the inner hot walls of which they move and undergo decomposition. Mass balances show in all the cases, a very low fraction of char (< 4 %) while the gasification yield increases with wall temperature  $T_W$ . It appears from figure 5 that the reaction seems to occur only for wall temperatures greater than about 800 K in good agreement with fusion temperature of 739 K. In such a model, the decomposition temperature of particles being roughly constant, the gasification yield increase with  $T_W$  would then result from further vaporization and/or decomposition of primary products (mainly liquids) at the wall and/or in the gas phase with an efficiency depending on  $T_W$ .

#### DISCUSSION

All these results obtained in different experimental conditions, show striking similarities between ablative wood pyrolysis and melting of solids. Nevertheless the equivalent fusion temperature of 739 K has been calculated from relation (4) based on the assumption that  $T_d$  is constant. Let suppose now that  $T_d$  depends on external physical conditions ( $p$ ,  $T_W$ ) under the assumption that  $\Delta H \ll v \rho_s Cp_s (T_d - T_0)$ . The heat flux density balance equation is :

$$h(T_W - T_d) = \rho_s Cp_s v (T_d - T_0) \quad (7)$$

The reaction occurring in ablation condition concerns only a thin external wood layer  $e$  inside which the equation of mass balance  $ke = v$  associated with  $ev = \alpha_s$  [5] leads to a relationship between the ablation velocity and the chemical first order kinetic constant  $k$  :  $k = v^2/\alpha_s$  and finally to :

$$T_d = \frac{h T_W + T_0 \sqrt{k \lambda_s \rho_s Cp_s}}{h + \sqrt{k \lambda_s \rho_s Cp_s}} \quad (8)$$

Figure 6 shows the variations of  $T_d$  with  $T_w$  ( $\lambda_s = 0.2 \text{ W m}^{-1} \text{ K}^{-1}$ ;  $C_{p_s} = 2800 \text{ J kg}^{-1} \text{ K}^{-1}$ ;  $\rho_s = 700 \text{ kg m}^{-3}$ ) with  $h$  as a parameter. The first order rate constant for the formation of "active cellulose" [9]  $k(\text{s}^{-1}) = 2.83 \times 10^{19} \exp -29000/T_d$  has been supposed to fit the present case of wood primary decomposition.

It can be observed that the smaller the values of  $h$ , the shortest the domain of wall temperature where  $T_d = T_w$  (for the lowest values of  $h$ ,  $T_d/T_w$  becomes less than one as wood begins to decompose). In most of usual experimental devices wood temperature is then very different from source temperature. Consequently, the direct determination of pyrolysis rate laws would have sense only for low wall temperatures ( $< 750 \text{ K}$ ).

Figure 6 shows that  $T_d$  varies with  $T_w$  and  $h$  indicating that strictly speaking, the fusion model is not appropriate. But it can be observed (specially for the low  $h$ ) that as soon as  $T_d/T_w < 1$ ,  $T_d$  increases more and more slowly with  $T_w$  and rapidly reaches a roughly constant value. Fusion model seems then to be an excellent first approximation.

The hatched zone reported in figure 6 is bounded by the extreme values of  $h$  determined in ref. [5] and by the extreme values of  $T_w$  explored. The "fusion temperature" of  $739 \text{ K}$  appears to be well situated inside the hatched surface. Such a fair agreement shows that the chosen kinetic law is a good approximation for wood decomposition. The "fusion temperature" must then be considered a mean value lying roughly between  $660$  and  $725 \text{ K}$  for  $T_w = 773 \text{ K}$  and between  $700$  and  $800 \text{ K}$  for  $T_w = 1173 \text{ K}$ .

## CONCLUSION

The behaviour of wood rods undergoing ablative pyrolysis by more or less intimate contact with a hot surface has revealed strong similarities with a phase change phenomenon. The principal reasons developed are the followings : quite similar behaviour of wood rods with true melting solids when applied on moving or fixed surfaces : same orders of magnitude of  $v$  and  $h$  ; same dependance law with applied pressure with a power  $F$  showing probable low values of the enthalpy of reaction ; same  $p^{0.25}$  dependance of  $v$  in the case of fixed surface ; same low of variations of  $v$  with wall temperature. Ablative pyrolysis carried out with sawdust in a cyclone reactor proves that no fast reaction occurs for wall temperatures lower than  $\sim 800 \text{ K}$ .

A consequence of these conclusions is that the accurate direct determination of kinetic rate constant of wood decomposition is a difficult task, likely impossible over wide ranges of temperatures in most of experimental devices (upper limit around about  $800 \text{ K}$ ). Even if such high temperatures could be reached, the system should be designed in such a way that the products of the reaction could also be removed from the reacting surface with high efficiencies. For example, figure 6 shows that  $T_d = T_w = 800 \text{ K}$  would be observed for  $h = 10^6 \text{ W m}^{-2} \text{ K}^{-1}$ . Assuming that the available heat flux is controlled by conduction through the oil layer, such a heat transfer coefficient would be effective for an equivalent layer thickness of  $0.1 \mu\text{m}$  ! (calculation made with a thermal conductivity of  $0.1 \text{ W m}^{-1} \text{ K}^{-1}$  for oil). Of course, an efficient removal of these liquids would prevent also the extent of their subsequent decomposition to secondary products and then to reduce the formation of new thermal isolating layers.

All these conclusions are in agreement with the analysis of other authors. Diebold pointed out in 1980 the efficiency of "solid convection" for carrying out the reaction of ablative pyrolysis of biomass (demonstration of

"sawing" biomass [4]. The same author stated also recently that cellulose passes probably through a liquid or plastic unstable state ("active cellulose") during pyrolysis before further decomposition [14] in agreement with Antal who points out the strong analogies observed between cellulose pyrolysis at high heating rates and phase change phenomena [10,11] with an upper limit at which pyrolysis occurs of 773 K. Evidence of such an upper limit is explained by a competition between heat demand from biomass and available external heat flux [12]. The same author [12] notices also the difficulty and indeed impossibility of achieving conditions whereby pyrolysis kinetics could be studied at very high temperatures. Finally, it must be reminded that in 1980, Reed [13] proposed a model for estimating the enthalpy of flash pyrolysis of wood based on several steps : heating of biomass up to a reaction temperature of 773 K, followed by a depolymerisation to form a solid which subsequently melts, melted matter being afterwards able to vaporize, following the temperature.

#### NOMENCLATURE

a	Constant ( $m s^{-1} Pa^{-F}$ )
Cp	Specific heat capacity ( $J kg^{-1} K^{-1}$ )
e	Thickness of reacting wood layer (m)
F	Exponent
h	Heat transfer coefficient ( $W m^{-2} K^{-1}$ )
H	Specific enthalpy ( $J kg^{-1}$ )
K	Constant ( $W m^{-2} K^{-1} Pa^{-F}$ )
k	First order kinetic constant ( $s^{-1}$ )
L	Heat of fusion ( $J kg^{-1}$ )
p	Pressure (Pa)
p <sub>o</sub>	Atmospheric pressure (Pa)
P	Reduced pressure
Pe	Peclet number
Ph	Phase change number
R	Radius of the solid cylinder (m)
T <sub>d</sub>	Wood surface temperature (K)
T <sub>f</sub>	Fusion temperature of a melting solid (K)
T <sub>o</sub>	Ambient temperature (K)
T <sub>w</sub>	Wall temperature (K)
v	Ablation velocity of the solid cylinder ( $m s^{-1}$ )
X	Gasification yield
V	Reduced velocity
α	Thermal diffusivity ( $m^2 s^{-1}$ )
λ	Thermal conductivity ( $W m^{-1} s^{-1}$ )
μ	Viscosity (Pa s)
ρ	Density ( $kg m^{-3}$ )

#### Subscripts :

s	solid cylinder
ℓ	liquid layer

#### REFERENCES

1. J. VILLERMAUX, B. ANTOINE, J. LEDE and F. SOULIGNAC. Chem. Eng. Sci. 41 (1986), 151
2. J. LEDE, F. VERZARO, B. ANTOINE and J. VILLERMAUX. Chem. Eng. Process, 20 (1986), 309
3. J. LEDE, F. VERZARO, B. ANTOINE and J. VILLERMAUX. Proceedings of Specialists Workshop on Fast Pyrolysis of Biomass, Copper Mountain Co, October 1980, p. 327

4. J.P. DIEBOLD, As Ref. 3, p. 237
5. J. LEDE, J. PANAGOPOULOS, H.Z. LI and J. VILLERMAUX. Fuel, 64 (1985), 1514
6. J. LEDE, H.Z. LI, J. VILLERMAUX and H. MARTIN. J. Anal. Appl. Pyrolysis, in press.
7. H. MARTIN, J. LEDE, H.Z. LI, J. VILLERMAUX, C. MOYNE and A. DEGIOVANNI. Int. J. Heat Mass Transfer, 29 (1986), 1407
8. H.Z. LI. Pyrolyse éclair de baguettes de bois. Modèle de fusion. DEA, (INPL, Nancy)(1984)
9. A.G.W. BRADBURY, Y. SAKAI and F. SHAFIZADEH. J. Appl. Polym. Sci., 23 (1979), 3271
10. V. KOTHARI and M.J. ANTAL. Fuel, 64 (1985), 1487
11. M.J. ANTAL. Fuel, 64 (1985), 1483
12. M.J. ANTAL. Biomass Pyrolysis. A review of the literature. Part 2 : Ligno-cellulose Pyrolysis. In Advances in Solar Energy, Plenum Press, New York vol. 2 (1985)
13. T.B. REED, J.P. DIEBOLD and R. DESROSIERS, As Ref. 3, p. 7
14. J.P. DIEBOLD. Thesis, T-3007, Colorado School of Mines, Golden, Co USA 80401 (1985)

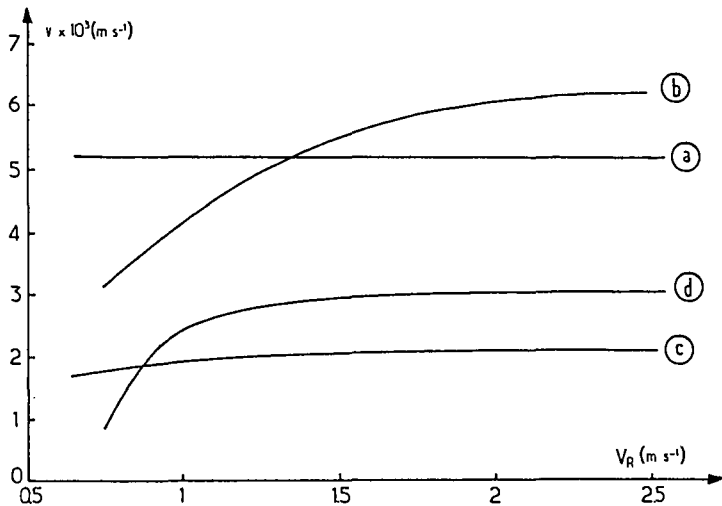


Fig. 1. Experimental variations of ablation velocities  $v$  with disk velocity  $V_R$  for four kinds of solids : a(ice,  $T_W = 348 \text{ K}$ ,  $p = 2 \times 10^5 \text{ Pa}$ ), b("rilsan",  $T_W = 723 \text{ K}$ ,  $p = 3,45 \times 10^5 \text{ Pa}$ ), c(paraffin,  $T_W = 373 \text{ K}$ ,  $p = 3,45 \times 10^5 \text{ Pa}$ ), and d (wood,  $T_W = 1073 \text{ K}$ ,  $p = 3,7 \times 10^5 \text{ Pa}$ ) (From [8]).

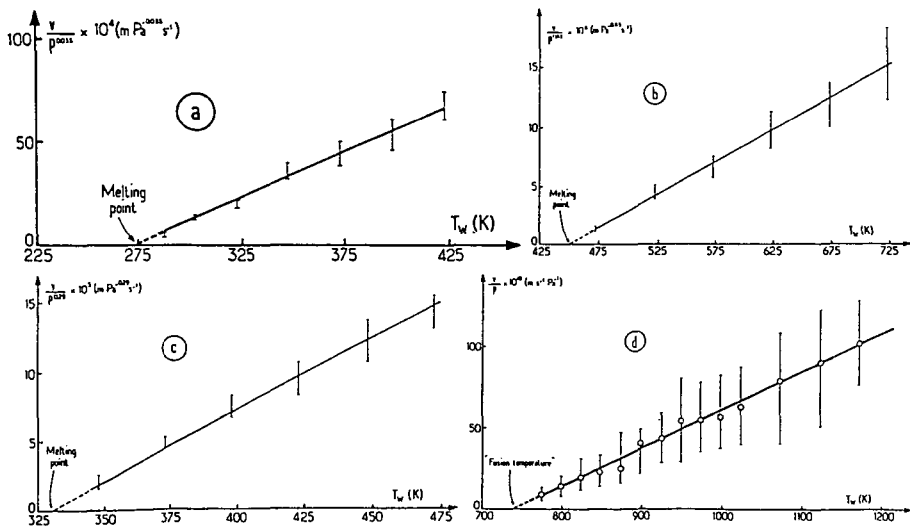


Fig. 2. Experimental variations of  $v/p^E$  with disk temperature  $T_W$  for : a(ice), b("rilsan"), c(paraffin) and d(wood) (From [8]).

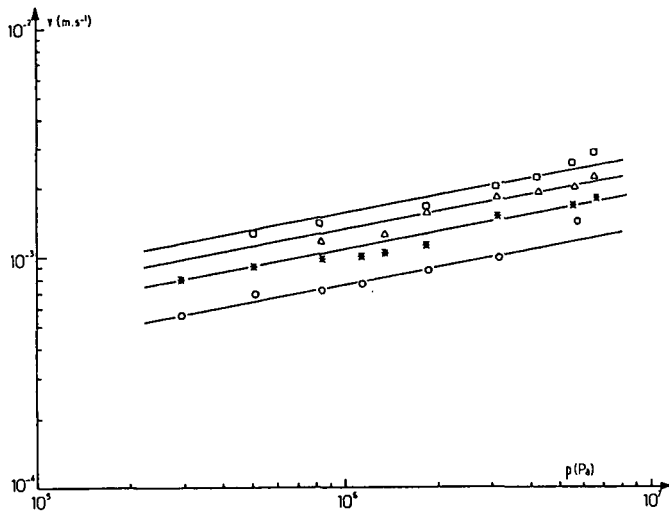


Fig. 3. Ablative pyrolysis rate of wood  $v$  as a function of applied pressure  $p$  for different wall temperatures -  $\circ$ : 823 K ;  $*$ : 873 K ;  $\Delta$ : 923 K ;  $\square$ : 973 K

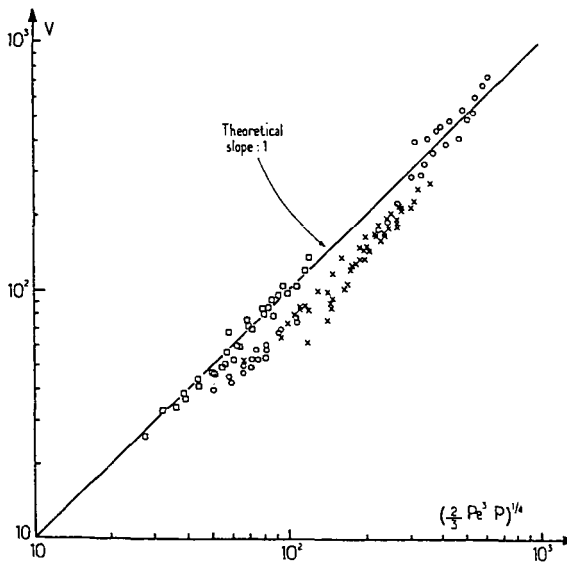


Fig. 4. Dimensionless representation of reduced velocity  $V$  as a function of reduced pressure  $P$  for three kinds of solids -  $\circ$ : paraffin ;  $x$ : ice ;  $\square$ : wood ...

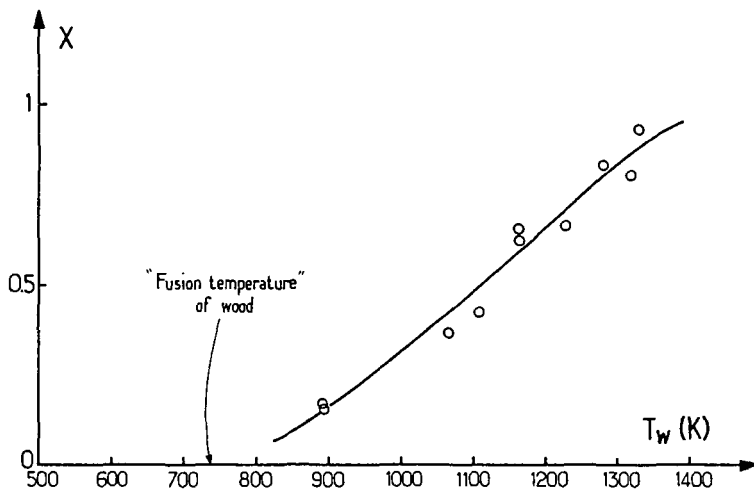


Fig. 5. Variation of the gasification yield  $X$  as a function of wall temperature  $T_w$  in the fast pyrolysis of wood sawdust in a cyclone reactor : comparison with the "fusion temperature" of 739 K.

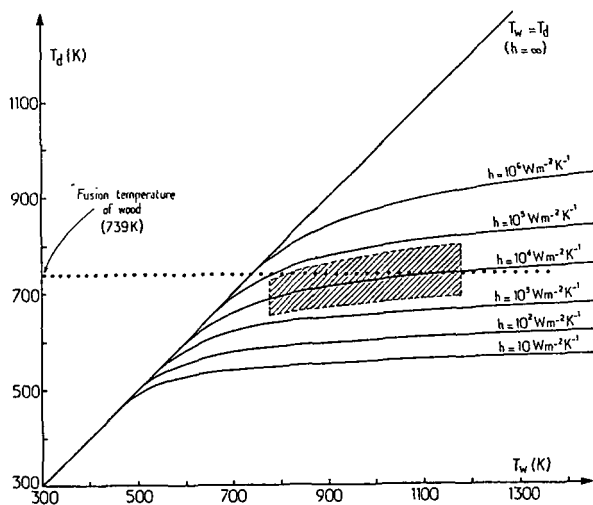


Fig. 6. Theoretical variations of wood surface temperature  $T_d$  as a function of heat source temperature  $T_w$  for different values of the external heat transfer coefficient. The hatched surface corresponds to the experimental domain ( $776 \leq T_w(K) \leq 1176$  and  $10^3 < h(W m^{-2} K^{-1}) < 6 \times 10^4$ ).

## HEAT FLUX REQUIREMENTS FOR FAST PYROLYSIS AND A NEW METHOD FOR GENERATING BIOMASS VAPOR

Thomas B. Reed & Craig D. Cowdery  
Colorado School of Mines, Golden CO 80401

### ABSTRACT

The term "fast pyrolysis" has been used to describe a pyrolysis regime in which vapor production is enhanced and char minimized by rapid heating. It has been found in the last decade that high yields of primary pyrolysis oil can be achieved using fast pyrolysis. More recently it has been found that the pyrolysis vapors can be converted to high grade fuels using a catalyst. This makes fast pyrolysis of biomass desirable for synthetic fuel manufacture.

We present here results derived from the Diebold Integrated Kinetic Model (DKM) that predict the time, the temperature, and the products of pyrolysis and the heat for pyrolysis of cellulose as a function of heating rates between 0.01 and 10<sup>5</sup>°C/min. This range covers very slow pyrolysis requiring days to fast pyrolysis occurring in fractions of a second. The predictions are in good qualitative agreement with experimental measurements.

We then compare the heat flux required for slow and fast pyrolysis for particles with that which can be obtained with practical heating devices. The comparison shows that convective and radiative heat transfer is adequate for fast pyrolysis of small particles, but not for large particles, due to conduction to the interior. We derive the heat flow requirements for large bodies, the time for onset of pyrolysis, and the depth of heat penetration in that time. We compare the heat flux from various practical devices with those observed in "contact pyrolysis" experiments of Diebold and Lede on large particles. The comparison shows that higher heat flux methods are required for fast pyrolysis of larger particles.

We have designed a "heat flux concentrator", based on the experiments of Diebold and Lede to generate wood vapors for upgrading to gasoline-like liquids. A rotating birch dowel is fed into a heated copper block. Vapors emerge from the bottom and are condensed and collected, or passed over a catalyst to establish optimum conversion conditions. The pyrolysis rates and results of catalytic conversion in these experiments will be described.

### INTRODUCTION

Pyrolysis of biomass is a very old and complex process producing variable quantities of charcoal, pyrolysis liquids and gases from biomass, peat or coals (1). Pyrolysis was the principle source of chemicals in Western society for about a century and could gain become a major source, particularly if the products can be tailored to modern needs through better understanding of the pyrolysis process or improved upgrading of the products.

The relative amounts of charcoal, liquid and gas obtained from pyrolysis depend on the time-temperature-pressure history of the sample in a way which may never be completely understood. This has led to apparent controversy over the magnitudes of kinetic factors, energies and products when investigators compare results from different experiments. Nevertheless great progress has been made in the last decade in understanding the role of these variables in controlling the nature and quantity of the products.

The term "fast pyrolysis" has been used to describe a pyrolysis regime in which vapor production is maximized and the formation of char is minimized by rapid heating. It has been found in the last decade that it is possible to obtain high yields of pyrolysis oils or

gas using high heat flux (1-3). It has more recently been found that pyrolysis oil can be converted catalytically to high grade, high octane motor fuel. Thus there is a strong motivation to understand these relations.

While there is no hard boundary between "slow" and "fast" pyrolysis, it is necessary to understand the relation between the time and energy required for each and the different chemistry and the possible mechanisms available for supplying this heat. We hope this paper will help draw together the apparently disparate results using a time-temperature-pressure kinetic model and lead toward more effective methods of pyrolysis.

### CELLULOSE AND BIOMASS PYROLYSIS KINETICS

Biomass is a composite plastic, consisting of cellulose, hemicellulose and lignin with cellulose constituting more than half the total and giving most of the mechanical strength. Cellulose has the best defined structure and thus has been studied more than lignin or hemicellulose. Furthermore it constitutes more than half the substance of most biomass and contributes most of the strength. Much of the following discussion applies primarily to cellulose, but qualitatively to all biomass.

The rates of pyrolysis reactions are usually represented in the form of a first order Arrhenius rate equation

$$dX/dt = -X A \exp(-E/RT) \quad 1)$$

where X represents the quantity of any reactant X at time t and temperature T. (A is the pre-exponential and E is the activation energy. R is the gas constant). If the biomass is heated at a constant rate of R °C/sec, simple substitution leads to

$$dX/dT = (-AX/R) \exp(-E/RT) \quad 2)$$

The values for A and E in Eqs. 1 and 2 are usually measured by thermogravimetric analysis (TGA) and describe the global pyrolysis (including all solid state reactions) in terms of a single A-E pair (2,3). While this oversimplification may be justified over a narrow temperature range for engineering purposes, the global approach ignores preliminary solid state reactions and thus is not able to predict the change of products with heating rate, the time required for pyrolysis or the temperature of pyrolysis.

Several reaction schemes for cellulose pyrolysis have been proposed involving competing parallel and consecutive reactions (2,3,5,6). Cellulose pyrolysis now appears to involve an initial drying step (not discussed here), followed by two parallel reactions which for instance differentiate between two subsequent paths as shown in Table 1. The first reaction involves cross linking (transglycolization) of the cellulose and leads to the formation of charcoal. The second reaction is a depolymerization leading to a low molecular weight liquid or solid depending on temperature and rate of formation. This was called the "active state" by Bradbury and Shafizadeh (4). These more volatile components may either immediately evaporate at low pressure or evaporate subsequently at higher pressures.

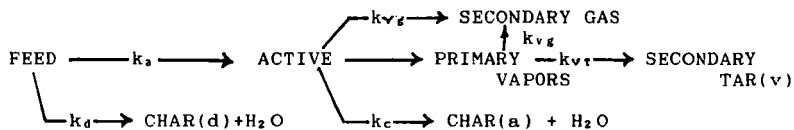
### AN INTEGRATED MODEL OF CELLULOSE BIOMASS PYROLYSIS KINETICS

The justification for studying the various pyrolysis reactions is to predict the detailed course of pyrolysis under a wide variety of conditions. Diebold has recently collected previous work on various aspects of cellulose pyrolysis into a single integrated model of cellulose pyrolysis (5,6). The six reactions included are shown in Table 1. The temperature at which the reaction rate reaches 10<sup>-6</sup>/s and 1/s is listed for convenience in evaluating the relative strength of each reaction. Note that the reaction producing char reaches a rate of

10<sup>-6</sup>/s at 208 °C, while the depolymerization reaction does not reach 10<sup>-6</sup>/s until 225 °C. Thus slow pyrolysis favors charring. However the depolymerization reaction reaches a rate of 1/s at 379 °C, while the charring reaction does not reach a rate of 1/s until 703 °C. Thus rapid heating favors depolymerization and volatilization over charring.

The Diebold Kinetic Model (DKM) permits calculation of the relative amounts of the products of pyrolysis as a function of time-temperature history. The kinetic equation 1) using values in Table 1 are integrated using the Runge-Kutta technique on a microcomputer. A second-derivative test is used to determine the time increment. The model permits any type of heating history, but the results given here are those for a constant heating rate as given in Eq. 2).

Table 1 - Simplified Cellulose Pyrolysis Reaction Scheme



REACTION	k	A sec <sup>-1</sup>	E KJ	T(R=10 <sup>-6</sup> ) °C	T(R = 1) °C
Cellulose to char + H2O	k <sub>d</sub>	6.69E+05	109	208	703
Cellulose to Active	k <sub>a</sub>	2.80E+19	243	225	379
Active to Primary Vapor at 1 atm	k <sub>v</sub>	6.79E+09	140	188	470
Active to primary vapor vacuum	k <sub>vv</sub>	3.20E+14	198	231	440
Active to Char(b) + H2O	k <sub>c</sub>	1.30E+10	153	224	518
Active to gas	k <sub>vg</sub>	3.57E+11	204	335	651
Primary vapors to gas	k <sub>vg</sub>	3.57E+11	204	335	651
Primary vapors to tars	k <sub>vt</sub>	1.81E+03	61	70	700

Notes: Kinetic constants used in Diebold kinetic model. T(R = 10<sup>-6</sup>) is the temperature where the rate constant R = 10<sup>-6</sup>; T(R = 1) is the temperature at which R = 1.

While this model may not explain all aspects of cellulose pyrolysis, it goes a long way toward predicting the changes observed with time-temperature-pressure. Other values for kinetic factors and other pathways should be substituted as they become known. In particular, an improved model should include the effect of pressure explicitly in the vaporization rates given by k<sub>v</sub> and k<sub>vv</sub>. The nature and role of the "active" state needs to be better defined, since it plays a key role in this and other schemes. We will use this model here to predict heat flux requirements for slow and fast pyrolysis of cellulose.

#### DEPENDENCE OF TIME, TEMPERATURE AND PRODUCTS ON HEATING RATE

The dependence of the pyrolysis time, t<sub>p</sub> and pyrolysis temperature, T<sub>p</sub> on heating rate predicted by the DKM are shown in Table 2 and Fig. 1. The dependence of products on heating rate is shown in Fig. 2. (It is the nature of an exponential decay that it is never complete. We have therefore arbitrarily taken the time and temperature of pyrolysis as that time and temperature where the reaction is more than 99.9% complete.)

Table 2 - Cellulose Pyrolysis Time, Temperature and Products  
 predicted by Kiebold Kinetic Model

PYROLYSIS CONDITIONS			PYROLYSIS PRODUCTS		
R Heat Rate R-°C/min	t <sub>p</sub> Pyr Time sec	T <sub>p</sub> Pyr Temp °C	Char- coal-%	Oil,Gas %	Water %
0.01	1650000	275	23.9	46.2	29.9
0.1	181200	302	12.4	73.2	14.9
1	19800	330	6.9	84.6	8.7
10	2142	357	4.2	90.3	5.4
100	234.6	391	2.6	94.3	3.1
1000	25.5	425	1.2	97.2	1.5
10000	2.778	463	0.005	98.7	0.007
100000	0.3042	507	0.003	99.4	0.003

Notes: Values calculated from Diebold model.

Here it is seen that pyrolysis temperatures vary between 280 and over 500°C as heating rates increase from 10<sup>-2</sup> to 10<sup>5</sup> °/min. In slow "commercial" pyrolysis, char yields are still increasing with pyrolysis times of over a month, and pyrolysis is complete at temperatures below 300°C. These correspond to the conditions that have been used classically for the manufacture of charcoal (1). Most of the kinetic data of Table 1 were acquired in experiments using convenient "laboratory" heating rates of 1-100°C/min. The predicted char yields of 2.6-6.9% and temperatures of 330-390°C correspond to those observed experimentally in this range.

At even higher "heroic" heating rates, gas and oilyields are still increasing with rates of over 10<sup>4</sup> °C/min where pyrolysis occurs at about 460°C. These conditions correspond to the experimental conditions of Diebold, Lede and Reed (7-9) produced by contact pyrolysis (see below). Thus it is clear that heating rate is a primary variable for controlling products in pyrolysis.

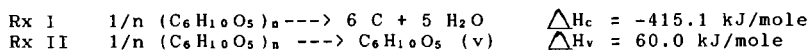
While the calculations in this paper are for cellulose, we believe the conclusions are qualitatively valid for all biomass.

#### HEAT OF PYROLYSIS AND HEAT FOR PYROLYSIS:

The energy required for pyrolysis,  $\Delta h_p$ , has long been a subject of interest to those involved in pyrolysis; yet no commonly accepted value is available to an engineer wishing to design a pyrolysis reactor, and even now it is not clear from the literature whether pyrolysis is endothermic or exothermic. It has been reported to vary from +370 J/g (endothermic) to -1700 J/g (exothermic)(5). One reason there is no commonly accepted value is that it is a difficult measurement to make under many of the conditions of pyrolysis (very slow or very rapid heating, large quantities of condensable vapors present, large temperature gradients in the sample). A more fundamental reason however is that the value depends on the particular form of biomass, the conditions of the experiment and the products formed, so that there is a unique value for each experiment. We will give here a method of calculating the heat of pyrolysis for known heating rates and products which, while approximate, underlines the factors that must be taken into account.

We define the "heat of pyrolysis" of biomass,  $\Delta h_p$ , as that heat required to effect the phase change from biomass to char-liquid-gas at

the temperature where pyrolysis occurs. (We define the "heat of pyrolysis as the heat required for the phase change plus the heat required to reach this temperature - see below.) A thermodynamic calculation of  $\Delta h_p$  can be made for cellulose based on the idealized reactions shown in Table 1. The idealized charring reaction for cellulose can be written as Rx I:



(Here we use the notation  $1/n (\text{C}_6\text{H}_{10}\text{O}_5)_n$  for cellulose to emphasize its polymeric nature. The values above are calculated from the heats of combustion or formation of the products and reactants.) The second reaction represents the depolymerization of cellulose to levoglucosan, with simultaneous vaporization. (Levoglucosan is the principal decomposition product of cellulose.)

These two reactions can be combined in the appropriate ratio to give a value for the heat of pyrolysis depending on the relative amount of carbon formed, eg

$$\begin{array}{l} \Delta H_p = 59.96 - 475.1 F_c \text{ kJ/mole} \quad 3) \\ \text{or} \quad \Delta h_p = 370 - 6603 F_c \text{ J/g} \quad 4) \end{array}$$

where  $F_c$  is the weight fraction of carbon produced in the charring reaction. These values of the heat of pyrolysis should be considered as idealized because pyrolysis of cellulose gives charcoal (not exactly carbon) and other products beside levoglucosan. Nevertheless they illustrate the necessity for knowing the products in measuring the heat of pyrolysis.

Antal recently used a high pressure scanning calorimeter to measure the  $\Delta h_p$  of cellulose (2). He varied the amount of char formed by changing the pressure of the experiment. He found an approximately linear change in the  $\Delta h_p$  of cellulose from -170 kJ/g with a char production of 23% (typical of slow pyrolysis) to +270 kJ/g with a char production of 9% (typical of fast pyrolysis)(5).

These values can be used in a linear equation to predict the heat of pyrolysis on the basis of char content  $F_c$ , ie

$$\Delta h_p = 553 - 3142 F_c \text{ kJ/g} \quad 5)$$

where  $F_c$  is the fraction of charcoal produced. Note that the values for the coefficients resulting from the experimental values are similar in magnitude to those predicted from thermodynamic calculation in Reaction 4). The heats of pyrolysis calculated from the predicted char production and pyrolysis temperatures are listed in Table 3.

A quantity of more interest to the engineer is the heat for pyrolysis. We define the "heat for pyrolysis",  $h_p$  as the sensible heat required to raise a biomass particle to pyrolysis temperature, ( $= c T_p$ , where  $c$  is the heat capacity of the biomass) plus the heat required to pyrolyse it,  $\Delta h_p$ . (If the products of pyrolysis are then heated above this temperature, this heat must also be included.) Table 3 also shows values of  $h_p$  for pyrolysis of cellulose calculated from 2) and the heat capacity of cellulose, 1.31 J/g-°C (0.32 Btu/lb-F). Note that the variation of  $h_p$  with heating rate is small compared with the variation of  $\Delta h_p$ .

Table 3 - Heat of Pyrolysis and Heat For Pyrolysis of cellulose Calculated from char production

PYROLYSIS CONDITIONS Heat Rate R-°C/min	Pyr Temp °C	Char-coal-%	$\Delta h_p$ J/g	$h_p$ J/g
0.01	275	23.9	-198	162
0.1	302	12.4	163	559
1	330	6.9	336	769
10	357	4.2	421	889
100	391	2.6	471	984
1000	425	1.2	515	1072
10000	463	0.005	553	1159
100000	507	0.003	553	1217

Notes: Char yield calculated from Diebold Model.  $\Delta h_p$  calculated from  $\Delta h_p = 553 - 3142F_c$ ;  $h_p$  calculated from  $h_p = \Delta h_p = c(T_p - T_o)$  with  $c = 1.3 \text{ J/g-}^\circ\text{C}$  for cellulose

HEAT FLUX REQUIRED FOR SLOW AND FAST PYROLYSIS  
A. Small Particles & Slow Heating

The average heat flux required to pyrolyse a particle is given by

$$\dot{q} = \Delta h_p \rho V / t_p A \quad (6)$$

where  $\dot{q}$  is the rate of heat supply per unit area,  $\rho$  is the density,  $V$  is the volume and  $A$  is the heated surface area of the particle. If the particle is a cube, this simplifies to

$$\dot{q} = h_p \rho L / 6 t_p \quad (7)$$

where  $L$  is the length of the cube edge.

The data in Table 2 and 3 can be combined with this equation to predict the magnitude of heat flux required for slow and fast pyrolysis. Table 4 shows the heat flux required to pyrolyse a 1 cm cube of cellulose (or biomass). The values shown are calculated for heating the particle just to pyrolysis temperature. They assume that the particle is approximately isothermal and pyrolysis occurs everywhere at once.

The above calculation assumes that there is no resistance to heat transfer, and the particle will be essentially isothermal. However most forms of wood and biomass are relatively poor conductors of heat and at higher heating rates the results shown above will not be valid. The validity of these assumptions is tested by the Biot number, given by

$$N_b = \text{Heat flux to surface/Heat flux to interior} \\ N_b = H L / K \quad (8)$$

(where  $H$  is the heat transfer coefficient, characteristic of whatever method of heating is used;  $L$  is a characteristic length of the particle, typically the cube root of the volume; and  $K$  is the thermal conductivity.)

Unfortunately the heat transfer coefficient  $H$  is generally applied to convection or radiation heating with small temperature differences, where heat transfer is a strong function of  $\Delta T$ . However for high temperature radiation and contact pyrolysis sources, the

change in  $\Delta T$  is relatively small and the Biot number is approximated by

$$N_B = \frac{\dot{q}L}{K\Delta T} \quad 9)$$

The maximum heat transfer coefficients for the various heating mechanisms are also shown in Table 6.

Table 4 - Heat flux requirements and Biot number for heating of a 1 cm cube

PYROLYSIS CONDITIONS					
R	T <sub>p</sub>	h <sub>p</sub>		$\dot{q}$	N <sub>B</sub>
Heat Rate	Pyr Temp			to 1 cm <sup>3</sup>	Biot No.
R-°C/min	°C	J/g		W/cm <sup>2</sup>	
0.01	275	162	:	8.20E-06	7.1E-06
0.1	302	559	:	2.57E-04	2.2E-04
1	330	769	:	3.23E-03	2.8E-03
10	357	889	:	0.035	0.030
100	391	984	:	0.35	0.304
1000	425	1072	:	3.50	3.0
10000	463	1159	:	34.78	30.2
100000	507	1217	:	333.41	289.9

Note: Heat flux calculated from  $\dot{q} = h_p \rho L/6 t_p$   
 Biot number calculated from  $N_B = h_p \rho L^2/6 t_p K \Delta T$   
 $K = 0.0023 \text{ J/s-cm-}^\circ\text{C}$

For Biot numbers less than 1, the particle will be nearly isothermal and will dry, then pyrolyse in sequence. For Biot numbers larger than 1, the resistance to heat transfer within the particle becomes large compared to that of the heat source and steep gradients exist in the particle. In this case the pyrolysis wave travels from the outside of the particle to the inside, producing simultaneous drying and pyrolysis.

The Biot number for a 1 cm cube is also shown in Table 4, calculated for the particle heating rates shown and assuming an average temperature difference of 500 K in. Here it can be seen that the assumption of an isothermal particle is valid for slow heating rates and small particles. However for a heating rate larger than 100 °C/min and a heating rate of 0.35 W/cm<sup>2</sup> there will be steep gradients in the particle, so that the heat flux will be altered and the drying and pyrolysis will occur simultaneously.

### B. Large Particles & Rapid Heating

For high heat flux and larger particles, when the Biot number exceeds 1, it is necessary to calculate the non-steady state heat transfer for the particular particle geometry and surface temperature. While this can be quite complex for most cases, it is relatively simple for the one dimensional steady state case experiment described by Lede in contact pyrolysis (8). In this case a heated disk supplies sufficient heat to a beech dowel to pyrolyse and vaporize it at a rate V. The steady state temperature distribution in the rod is given by

$$T(x) = T_0 + (q/\rho cV)\exp(-Vx/\alpha) = (T_d - T_0)\exp(-Vx/\alpha) + T_0 \quad 10)$$

where T(x) is the temperature at a distance x from the heat source of strength q, T<sub>p</sub> is the temperature at the pyrolysing interface and T<sub>0</sub> is the initial temperature of the rod. The density of the wood is  $\rho$ , c

is the heat capacity,  $\alpha$  the thermal diffusivity and  $V$  the rate of pyrolysis. (Here we have taken the following values used by Lede for consistency; heat capacity,  $c = 2.80 \text{ J/g-}^\circ\text{C}$ ; density =  $\rho = 0.70 \text{ g/cm}^3$ ; thermal conductivity  $\kappa = 0.0023 \text{ J/s-cm-}^\circ\text{C}$ ; thermal diffusivity =  $\alpha = 0.0012 \text{ cm}^2/\text{s}$

Table 5 - Steady State Fusion-Pyrolysis of Birch Rod

HEAT FLUX	$\dot{q}$	10.00	100	1000	W/cm <sup>2</sup>
Velocity (b)	$V$	0.01	0.11	1.14	cm/s
Penetration (c)	$X(1/e)$	0.10	0.01	0.001	cm
Heat stored	$Q$	89.76	8.98	0.90	J/cm <sup>2</sup>
Induction Time (e)	$t_i$	9.0	0.09	0.0009	s

Notes and assumptions: (a)  $T_p = 466 \text{ }^\circ\text{C}$ ,  $T_o = 20 \text{ }^\circ\text{C}$

(b) The pyrolysis velocity,  $V$  was calculated from  $V = q/(\rho c)(T_p - T_o)$

(c) The heat penetration  $X(1/e)$  was taken to be the distance at which the temperature had fallen to  $1/e$  of  $T_p$ ,  $VX/\alpha = 1$ ,  $X = \alpha/V$ .

(d) The heat stored in the rod,  $Q$ , was calculated as the integral of the sensible heat between  $x=0$  and  $x=\infty$ ,  $= \alpha c \rho (T_p - T_o)/V$

(e) The induction time  $t_i$  is the time required to establish the steady state temperature gradient,  $t_i = Q/\dot{q}$ . This assumes the heat transfer intensity is constant before steady state is reached.

(f) Temperature Distribution  $T = T_p \exp(-Vx/\alpha) + T_o$ .

Note in Table 5 that the velocity and heat penetration increase linearly with heat flux. However, the induction time required to reach steady state varies inversely as the square of heat flux. At low flux, considerable char may build at the interface so that the steady state condition may never be reached.

#### HEAT TRANSFER MECHANISMS FOR FAST PYROLYSIS

The magnitudes of heating rates which can be obtained from various methods of heat transfer are shown in Table 6 (Reed, 1981 Cu Mtn.). Comparing the fluxes shown in Table 4 to the values in Table 5, it can be seen that the high heating rates required for fast pyrolysis of small particles can be achieved with convection, radiation or conduction.

Convection is the least satisfactory heat transfer mechanism for fast pyrolysis because the water and pyrolysis vapors produced during pyrolysis interfere with heat transfer. Also convection from gas sources with temperatures above  $600 \text{ }^\circ\text{C}$  is unsuitable for oil production because they crack the pyrolysis oils which are only stable to about  $600 \text{ }^\circ\text{C}$ . Low temperature radiation sources (below  $1000 \text{ }^\circ\text{C}$  are also unsatisfactory for fast pyrolysis of larger particles.

The production of pyrolysis oil is favored by radiation from a high temperature source or by "contact pyrolysis" (see below). In the case of radiation, the solid is heated rapidly, but the vapors are largely transparent and transient and so are not overheated (12). Unfortunately black body sources with temperatures above  $2000 \text{ }^\circ\text{C}$  are expensive and difficult to use.

#### CONTACT PYROLYSIS

A new method of heat transfer, "contact pyrolysis", has been developed in the 1980's and appears to be especially suited for the production of pyrolysis oil vapor.

Table 6 - Heat Transfer Rates and Heat Transfer Coefficients from Various Devices

	Typical Temp diff $\Delta T$ K	Maximum Ht Transf $\dot{q}$ W/cm <sup>2</sup>	Maximum Ht tr coef H W/cm <sup>2</sup> -K
CONVECTION			
Gas Free Convection	500	10	0.02
Gas forced convection	500	300	0.6
Air-Gas Flame	1500	200	0.13
Oxy-Acetylene flame	3000	3000	1.00
CONVECTION, ELECTRONIC			
Electric arc	10,000	20,000	2
RADIATION			
	Surface T °K		
Black Body	773	20	0.026
	1,273	150	0.12
	2,273	1,500	0.66
	5,273	44,000	8.3
Focused CO2 laser		100,000	NA
CONTACT PYROLYSIS	873	3,000	3.2

In 1980 Diebold showed that a moving hot wire would cut through a piece of wood at rates of several cm/sec with apparently no production of charcoal (7). Ledè et al have since shown that a wood dowel can be consumed at rates up to 3 cm/sec corresponding to heat transfer rates of 3000 J/cm<sup>2</sup> by pressing it against a heated disk (8). Furthermore the heat transfer rate is directly proportional to pressure, and a pressure of 30 atmospheres was used to attain the above heat transfer rate. The heat transfer is also proportional to the difference between the disk temperature and 466 °C. This was interpreted to show that the wood had a "fusion behavior" above 466°C (8,13). Reed has now developed a "heat flux concentrator" (see below) using a copper block to produce vapors for catalytic conversion to fuel (9).

Contact pyrolysis has several interesting and non-obvious features:

- o The thermal conductivity of metals is typically 3-4 orders of magnitude higher than that of hot gases or biomass, and so the heat transfer produced by direct contact is proportionally high.
- o The use of pressure at the heated interface retards the vaporization of the pyrolysis products so that they do not interfere with heat transfer, and instead the biomass pyrolyses to an oil or foam
- o When the resulting oil or foam is squeezed out of the interface region, it is immediately in a low pressure region and can vaporize very rapidly
- o The rubbing contact removes char or ash which would otherwise interfere with heat transfer

**A HEAT FLUX CONCENTRATOR FOR CONTACT PYROLYSIS PRODUCTION OF PYROLYSIS OIL VAPOR**

In order to produce vapors for catalytic conversion to hydrocarbon fuels, we have developed a "heat flux concentrator" shown

in Fig. 5 and 6. In operation, a wood dowel is rotated in a drill press and forced into a 1.2 cm diameter tapered hole in the heated copper block shown in Fig. 5. The rod is fed at a rate of 0.2 - 0.25 cm/sec. The vapors escape through 12 holes through the bottom of the block and are then captured in traps and in a gas burette. Alternatively, the vapors travel without cooling to a catalyst test furnace as shown in Fig. 6 where the products are captured (9).

The heat flux concentrator has been operated to produce pyrolysis vapor as an end product, or to test the operation of various catalysts. A preliminary mass balance on pyrolysis oil production is shown in Table 7 for pyrolysis runs. We observe that the walls of the pyrolyser and the exit holes become coated with a hard, shiny form of carbon like petroleum coke. We now believe that there is a high resistance to vaporization which causes plugging of the pyrolyser after the feeding of about 5 g. We are currently modifying the design to improve vaporization. A few catalyst runs have also been made and they will be described in more detail later.

=====

Table 7 - Preliminary Mass Balance on Contact Pyrolysis Experiments

Pyrolysis Run	T <sup>p</sup> °C	Wood Consumed	g liq/ g wood	g gas/ g wood	g coke/ g wood	Mass out/ Mass in
5p	550	2.56	0.61	0.10	0.27	0.98
8p	600	5.59	0.57	0.10	0.33	1.00
9p	500	6.10	0.52	0.12	0.25	0.89
11p	700	4.21	0.57	0.13	0.14	0.85

=====

#### Acknowledgements

The authors would like to thank the Solar Energy Research Institute for support of this work under Contract HK-6-06059-1 and the Midwest Research Institute for thier support. The authors would especially like to thank their colleagues at SERI and elsewhere whose work has supplied the base on which this paper has been written.

#### REFERENCES

1. Stern, A. J. and Harris, E. E., "Chemical Processing of Wood", Chemical Publishing Co., New York, 1953
2. Antal, M. J., Jr., "Biomass Pyrolysis: A Review of the Literature, Part I-Carbohydrate Pyrolysis", in *Advances in Solar Energy*, ed K. W. Boer and J. A. Duffie, American Solar Energy Society, Boulder, CO, Vol 1, pp 61-112.
3. Antal, M. J., Jr., "Biomass Pyrolysis: A Review of the Literature, Part II-Lignocellulose Pyrolysis, in *Advances in Solar Energy*, ed K. W. Boer and J. A. Duffie, American Solar Energy and Plenum Press, New York, Vol 2, pp 175-255.
4. Bradbury, A. G., Sakai, Yoshio and Shafizadeh, F., "A Kinetic Model for Pyrolysis of Cellulose", *J. Appl. Polymer Science*, 23 3271 (1979)
5. Diebold, J. P., "The Cracking Kinetics of Depolymerized Biomass Vapors in a Continuous Tubular Reactor", Thesis T-3007, Colorado School of Mines, Golden, CO 1985.
6. Diebold, J. P., Scahill, "Ablative, Entrained Flow Fast Pyrolysis of Biomass", in *Proceedings of the 16th Biomass Thermochemical Contractors' Meeting*, Portland, OR May 8-9, 1984, PNL-SA-12403, 1984. See also, Diebold, J. P. "A unified Global Model for the Pyrolysis of Cellulose", (in preparation).
7. Diebold, J. P., "Ablative Pyrolysis of Macroparticles of Biomass," *Proceedings of the Specialists Workshop on the Fast Pyrolysis of Biomass*, Copper Mountain, CO., Oct. 12 1980, Solar Energy Research Institute, Golden, CO. 80401, SERI/CP-622-1096.
8. Lede, J., Panagopoulos, J., Li, H. Z. and Villiermaux, J., "Fast Pyrolysis of Wood: Direct Measurement and Study of Ablation Rate", *Fuel* 64, 1514 (1985)
9. Reed, T. B., Diebold, J. P., Chum, H. L., Evans, R. J. Milne, T. A. and Scahill, J. W., "Overview of Biomass Fast Pyrolysis and Catalytic Upgrading to Liquid Fuels," in *Proceedings of the American Solar Energy Society*, K. W. Boer, Ed., Boulder, CO June 11, 1986.
10. Roberts, A. F., "The Heat of Reaction During the Pyrolysis of Wood", *Combustion and Flame* 17, 79 (1971).
11. Reed, T. B., Diebold, J. P. and Desrosiers, R., "Perspectives in Heat Transfer for Pyrolysis", *Proceedings of the Specialists Workshop on the Fast Pyrolysis of Biomass*, Copper Mountain, CO., Oct. 12 1980, Solar Energy Research Institute, Golden, CO. 80401, SERI/CP-622-1096.
12. Chan, W. -C. R., Kelbon, M. and Krieger, B. B., "Product Formation in the Pyrolysis of Large Wood Particles", *Fundamentals of Thermochemical Biomass Conversion*, ed. R. P. Overend et al, Elsevier, New York, 1985.

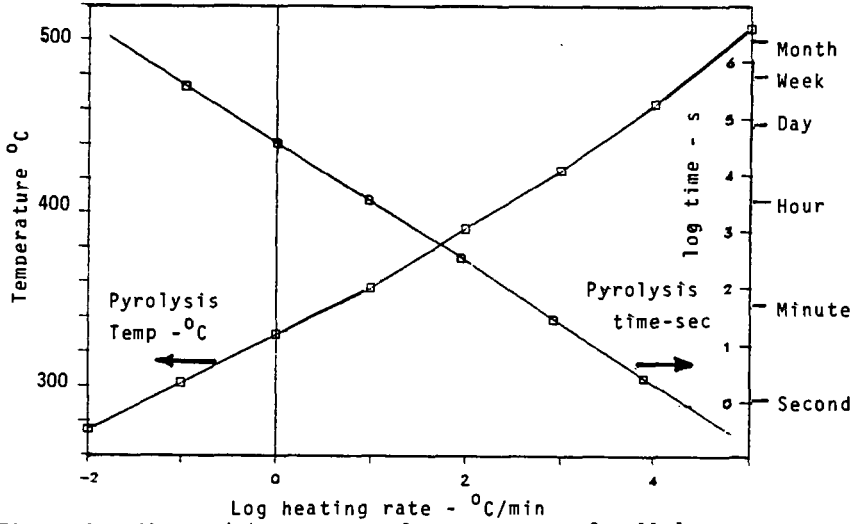


Figure 1 - Time and temperature for pyrolysis of cellulose as predicted by Diebold Kinetic Model

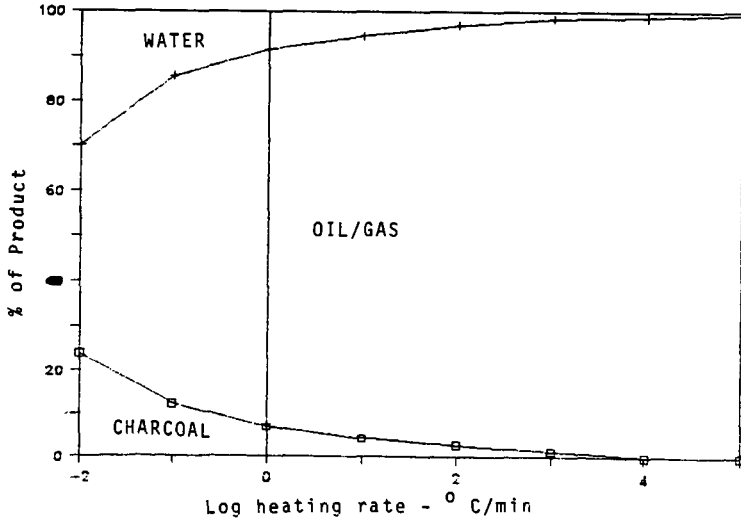


Figure 2 - Products of cellulose pyrolysis as predicted by Diebold Kinetic Model

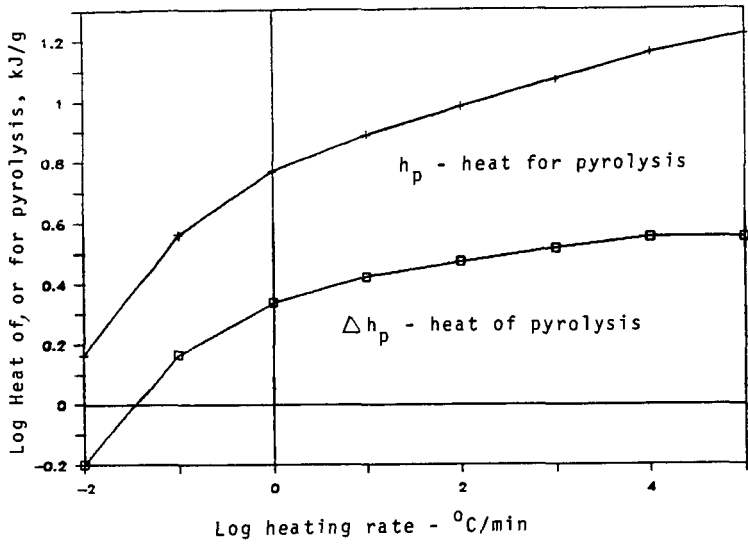


Figure 3 - Heat of pyrolysis and heat for pyrolysis as predicted from char yields and pyrolysis temperature

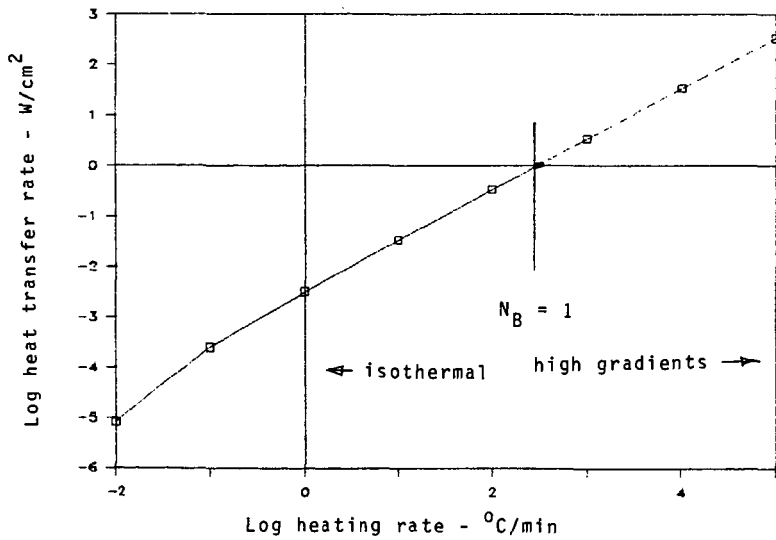


Figure 4 - Heat transfer rate required to support heating rate

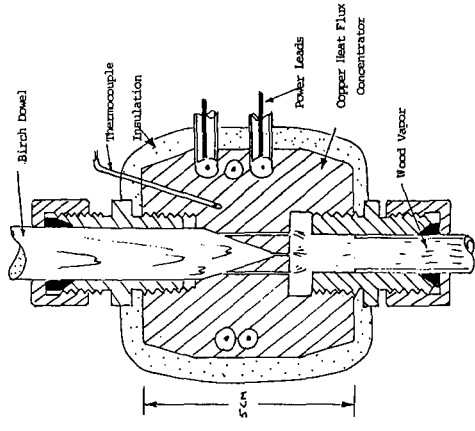


Figure 5 - Contact pyrolysis furnace for producing wood vapor.

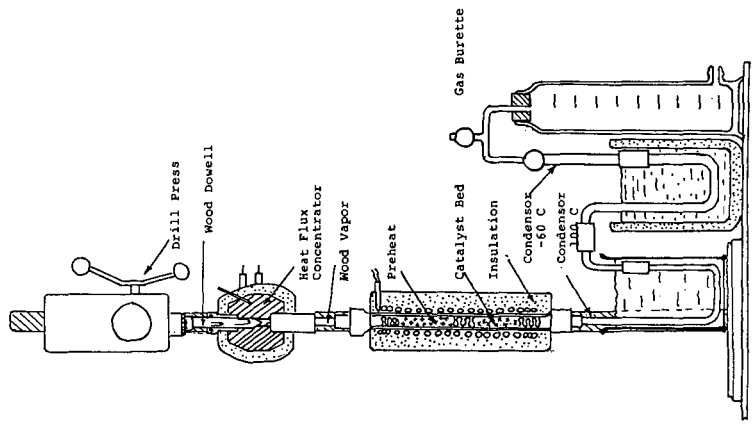


Figure 6 - Microanalytic test apparatus for catalyst testing

PRODUCTION AND CHARACTERIZATION OF PYROLYSIS  
LIQUIDS FROM MUNICIPAL SOLID WASTE

James E. Helt and Ravindra K. Agrawal

Argonne National Laboratory  
9700 S. Cass Ave.  
Argonne, IL 60439

INTRODUCTION

Municipal solid waste (MSW) is a highly variable "raw material," by both season and location. However, it is generally accepted to have a composition within the ranges shown in Table 1 (1). Cellulosic materials, including paper, newsprint, packaging materials, wood wastes, and yard clippings, constitute over 50% of MSW.

A basic understanding of the pyrolytic reactions is important and relevant to both combustion and conversion of MSW. As MSW is heated the different components react differently at different temperatures. The volatile species can evaporate without major change, and the rest of the cellulosic components partially break down to volatile components leaving a carbonaceous char that contains the ash and noncombustibles. The volatile pyrolysis products consist of a gaseous fraction containing CO, CO<sub>2</sub>, some hydrocarbons, and H<sub>2</sub>, which are noncondensables. There is a condensable fraction containing H<sub>2</sub>O, volatile hydrocarbons and low molecular weight degradation products such as aldehydes, acids, ketones, and alcohols. Finally, there is a tar fraction containing higher molecular weight sugar residues, furan derivatives, and phenolic compounds. The proportion and composition of these products are highly dependent on the cellulosic composition of the MSW, the pyrolysis temperature and the presence of inorganic compounds that could influence (catalyze) the pyrolysis reactions.

Pyrolysis of cellulose at temperatures below 300°C results mainly in char formation. Any lignin present in the MSW (Kraft paper, cardboard, and wood waste contain significant proportions) has a higher tendency for charring, whereas the cellulose and hemicelluloses readily decompose to volatile products at temperatures above 300°C. Most of the plastics present thermally degrade at a significantly higher temperature (400-450°C) (2).

BASIC MECHANISMS RESEARCH

The ANL/DOE program on pyrolysis of municipal solid waste (MSW) has two overall objectives: (1) to understand the basic thermokinetic mechanisms associated with the pyrolytic conversion of MSW and (2) to seek new processing schemes or methods of producing a liquid or gaseous fuel from MSW feedstock. To meet these objectives, we are performing laboratory experiments with the aim of determining the effects of different operating parameters on the pyrolysis-product compositions and deriving an analytical model of the pyrolytic process that describes the chemical kinetics.

This DOE-sponsored research has both ANL activities and subcontracted work. Argonne is performing closely controlled laboratory-scale parametric tests. The work is being performed on two experimental facilities: (1) a TGA to study the thermal degradation versus temperature, and (2) a bench-scale reactor to produce significant quantities of products to permit characterization. The goal is to determine how different operating parameters influence the product compositions.

Subcontracted activities are being performed at the Solar Energy Research Institute (SERI) and the Chemical Engineering Department at the University of Arizona. SERI has used their direct high-pressure molecular beam mass spectrometric sampling system to collect qualitative "fingerprints" and experimental data on the pyrolysis products generated from components of MSW and various refuse derived fuel (RDF) samples (3). They are also using the same experimental apparatus to distinguish between the primary and secondary reactions leading to the formation of the pyrolysis products (4). This data will be part of an overall data base to describe the influence of sample properties and reaction conditions on the solid phase and gas phase processes of low-temperature (<500°C) MSW pyrolysis to oils. Additionally, SERI has recently started a new task on the development of a rapid method of characterizing the liquid products from pyrolysis based on mass spectrometric data. This new task is composed of three parts: 1) compound class analysis by advanced pattern recognition techniques, 2) liquid product analysis via compound class analysis, and 3) correlation of chemical composition to fuel properties.

The University of Arizona has completed a small research effort on the fundamentals of direct liquefaction of MSW (5). They modified an existing autoclave and a real-time digital microprocessor control system so that it could be operated in a semi-continuous mode. Various components of MSW were studied in order to obtain meaningful data, not confused by the different thermokinetics of more than one distinct MSW component. Feedstocks included wood flour, cardboard, newsprint and rice (starch), as well as the important model compounds alpha cellulose and lignin. It was found that these MSW components could be converted to liquid oils and a high-heating value residual solid at temperatures of 325°C to 400°C and pressures of 1000 psi to 3000 psi.

A task which is related to the basic mechanisms work is also being performed by ANL (2). This task explores the possibility of using catalytic hydrotreating to upgrade the liquid products produced during conventional pyrolysis of MSW. The liquid products obtained from MSW pyrolysis processes are generally unsuitable for use as liquid fuels. Heating values are low and the liquids are very corrosive, viscous and unstable during storage. A major reason for these problems is the extremely high oxygen content of the pyrolysis products. The kinetics of catalytic reactions that remove oxygen-containing compounds from the pyrolysis liquids is being experimentally determined in a high-pressure, fixed-bed microreactor of the trickle-bed type. The reactions of interest involve the reduction of the oxygen-containing hydrocarbon with high pressure hydrogen using a solid catalyst. The catalysts which have been used are primarily commercially available hydrodesulfurization (HDS) catalysts containing molybdenum oxide with either cobalt or nickel oxide, supported on high surface area alumina matrix.

#### ANL BENCH-SCALE STUDIES

The emphasis of this paper will be on the bench-scale studies being performed at ANL and on the associated activities in characterizing the liquids produced in the pyrolysis reactions.

The reactor is a fixed bed contained inside a quartz tube (70-mm ID) and placed between two glass frits. The outside of the tube is enclosed in a furnace. The reactor tube can be purged from top to bottom with the desired gas(es). The reactor is operated in the nonisothermal mode with heatup rates as high as 30°C/min. Temperatures are recorded on a multipoint recorder to allow indication of existing temperatures and temperature gradients. There is a rotameter on the inlet gas line and a dry gas meter on the outlet. Cold traps are in the gas outlet downstream of the condenser unit. These traps are filled with ice or dry ice. Downstream of the traps, the gases that do not condense are collected in plastic sampling bags for analysis by gas chromatography (GC).

Experimental results on the thermal decomposition of typical MSW components (Whatman #1, newsprint, kraft paper, cardboard, aspen, and pine) over a temperature range of 275-475°C have been gathered. The details of these experimental runs may be found elsewhere (6). Also, information on the TGA runs used in support of this bench-scale work is available elsewhere (7,8).

#### CHARACTERIZATION OF LIQUIDS

Various liquid samples produced in the bench-scale apparatus have been analyzed with GC and GC/MS. The chromatograms were qualitatively compared to each other by both measurement of peak retention times and by observation of the patterns present. As a result, six different groups were identified:

- Group A - Most components elute early in the chromatogram as many sharp peaks within a small retention window.
- Group B - Bulk of components elute across a 6- to 20-min retention window and are a mix of both sharp and broad peaks.
- Group C - Many peaks are observed; the bulk of components elute across a 4- to 30-min retention window.
- Group D - Similar to C, but most components elute across a 4- to 20-min retention window.
- Group E - A few early peaks are observed, especially in the 5- to 7-min retention window.
- Group F - Similar to D, but many peaks are observed in the 9- to 11-min retention window.

The mass spectrum obtained from a typical tar sample is shown in Fig. 1. This tar sample was produced from a newsprint feedstock pyrolyzed in an inert atmosphere of helium. A computer search was performed using the 31,000 component NIH/EPA library in addition to a library of compounds from Battelle Pacific Northwest Laboratory (9). The results of the computer search and from interpretation of various standard spectra yielded tentative identification of numerous compounds. It is apparent that many compounds of homologous series are present. Recognition of just one of the compounds in a series leads to identification of all since they will most likely differ only by 14 amu (a CH<sub>2</sub> group) or by 31 amu (a CH<sub>3</sub>O group). In some cases the same identification is made for more than one compound. Actually, different isomers of the compound are probably being found. The percent found was estimated by dividing the response of the most abundant ion for a compound by the total of the responses of the most abundant ions for all compounds.

In general, the classes of compounds included furfurals (9.4%), phenols (2.5%), methoxyphenols (16.9%), cyclic compounds such as methyl cyclopentanones (10.8%), methoxy benzenes (3.8%), and the substituted propane tentatively identified for the peak at scan number 1207 (36.8%). Although the compound eluting at scan 1207 is by far in the highest concentration, insufficient information is available from its spectrum to allow a reasonable identification. The base peak observed is 75amu, and a 115 amu ion is also present at 40% abundance.

With the computerized mass spectral matching capability, a substituted propane with a molecular weight of 192 g/mol (propane, 1,3-dimethoxy-2,2-bis(methoxymethyl)) was selected as the most probable compound. The sample was submitted for gas chromatograph/matrix isolation/Fourier transform infrared (GC/MI/FTIR) analysis to add to the information necessary for better identification.

A GC/MI/FTIR run provided useful information on the bulk of the material present in the sample at scan number 1207. Data from the GC/MI/FTIR analysis indicated that the computerized mass spectral identification of the component eluting at scan number 1207 is not far off. The compound does not contain phenyl groups, and computerized IR searches came up with compounds with an ethanol/ethane or propanol/propane backbone substituted with methoxy or ethoxy groups. In particular, three close matches are dimethyl acetaldehyde,  $(\text{CH}_3\text{O})_2\text{-CH-CHO}$ ; 1-methoxy-2-propanol,  $\text{CH}_3\text{O-CH}_2\text{-CH(OH)-CH}_3$ ; and 1,3-diethoxy-2-propanol,  $\text{CH}_3\text{CH}_2\text{O-CH}_2\text{-CH(OH)-CH}_2\text{-OCH}_2\text{CH}_3$ . The presence of methoxy or ethoxy groups is consistent with the tentative identification given for the compound.

Another compound present in a relatively large concentration but which cannot be identified is that eluting at scan number 1343. This compound has an apparent molecular weight of 110 amu, with ions at 71, 89, and 110 amu. It appears to be neither a methyl furfuryl, benzenediol, nor dimethyl cyclopentanone. The 71-amu ion probably results from a  $\text{CH}_3\text{-CH}_2\text{-C=O}$  group, which can come from a tetrahydrofurfuryl structure or from a butyl ester. The compound's real molecular weight may be above 110 amu.

#### YIELDS AND ANALYTICAL RESULTS

With the Whatman No. 1 filter paper, the yields at 475°C of water vapor and gases were in the ranges 5-13 wt % and 26-34 wt %, respectively, of the original cellulose. The hydrogen balance suggests the higher water content (13%), whereas both the carbon and oxygen contents suggest a lower water yield (5 wt %).

Efforts have been made to analyze the gases collected in the sample bags. A Hewlett-Packard Gas Chromatograph is being used to identify major gas components. The preliminary GC analyses show that, for the Whatman No. 1 paper at 475°C, the gases produced are 56.6 vol%  $\text{CO}_2$  and 43.4 vol%  $\text{CO}$ . No other gases were detected in significant quantities. The yield of  $\text{CO}_2$  is, therefore, in the range of 18-23 wt % of the original cellulose and the yield of  $\text{CO}$  is 8-11 wt %. Roughly 25% of the energy in the feedstock is released in the gaseous products. These pyrolysis gases can be considered a low-Btu fuel.

The Whatman No. 1 paper (as received) contained 4.1 vol % moisture and 0.074 wt % ash. All results reported here are on a moisture-ash-free basis unless otherwise specified. Table 3 summarizes some analytical results of cellulose and condensed-phase cellulose pyrolysis products. A comparison of the results in Table 2 for cellulose and cellulose tars indicates that the elemental composition of these two materials is very similar. (The heating value of cellulose tars reported here may be low due to the loss of lower-molecular-weight products during the drying step.) Tars seem to have a slightly higher heating value than that of cellulose. These results strongly suggest that the nature of cellulose tars is similar to that of its parent cellulose.

As can be seen from Table 2, the cellulose chars are very different from the parent cellulose. When compared with the original cellulose, the cellulose chars have a carbon content that is roughly double, and  $\text{H}_2$  and  $\text{O}_2$  contents that are about one-half and one-third respectively. The richness in carbon content of the chars is indicated by their high heating value (7566 cal/g). Unfortunately, the low  $\text{H}_2$  content of the chars make them an unlikely candidate for use as transportation fuels. Because of the high carbon content and low  $\text{H}_2$  and  $\text{O}_2$  content, the cellulosic chars are comparable to a low-volatile bituminous coal or a low-grade anthracite coal. However, since the chars contain no sulfur or nitrogen compounds that could form potential air pollutants upon combustion, they do have potential as a solid fuel. Tables 3 and 4 give the analytical results for newsprint and Kraft paper feedstock.

The atomic ratios (H/C and O/C) and the heating value of cellulosic chars indicate that they are very similar to coal. The H/C ratio of cellulose tars (1.73) is comparable to that of No. 2 fuel oil (1.84). Unfortunately, the high oxygen content indicated by the O/C ratio (0.91 compared to 0.01 for fuel oil) significantly reduces the heating value of the tars.

#### DISCUSSION

It should be noted that the tar analysis results of this study are very similar to those obtained from vacuum pyrolysis of small cellulose samples conducted by Agrawal et al (10). Also the tar yields are comparable to those obtained by Shafizadeh (11) using small samples of Whatman No. 1 paper under vacuum conditions. These findings support the assumption that negligible tar decomposition takes place in the reaction bed.

Efforts are also in progress to ascertain some of the possible heat and mass transfer limitations of the pyrolysis process. Fig. 2 depicts the residue and tar yields of 5-g and 15-g cellulose samples at a heating rate of 5°C/min. Increased sample weight shifts the weight-loss curve to a higher temperature by about 10°C. Fig. 2 also shows that increased sample weight decreases the tar yields. Efforts to explain this effect of sample weight on product yield are in progress.

Figures 3 and 4 summarize the data for the influence of heating rate on product yields from Whatman No. 1 paper. It is seen from Figs. 3 and 4 that increasing the heating rate or sample weight has a similar effect in shifting the weight-loss curve to a higher peak temperature. However, the shift in the weight-loss curve along the peak-temperature axis in the case of increased sample weight is due to mass transfer limitations, whereas, in the case of increased heating rate, this shift is due to combined effects of kinetics and heat transfer resulting in delayed decomposition. At a peak temperature of about 370°C, the product yields are essentially independent of the heating rates (Fig. 4).

The results in Table 6 illustrate the influence of sample weight and heating rate on product yields. The data show that increasing sample size reduces the tar yields and increases the char yields. The drastic decrease in tar yields is primarily due to increased vapor residence time in the reaction bed. If the vapor residence time is reduced in the reaction bed by using a fluidized bed or an entrained flow reactor, then secondary decomposition can be significantly reduced, and the effects of sample weight will not be as drastic. Thus, data collected in the loosely packed fixed-bed reactor of the present study may represent an extreme for an operating industrial reactor.

Increasing the heating rate appears to decrease the char yields but has little influence on tar yields. This implies that gas yields increase at the expense of char yields.

Table 7 summarizes elemental analyses of chars formed under various pyrolysis conditions. The elemental analyses of cellulosic chars suggest that the composition of chars is not strongly influenced by either the heating rate or sample weight.

Results to date strongly imply that, depending on the residence time, the tar yields for final pyrolysis temperatures above 300°C will be independent of heating rates. This observation is strengthened by the finding from TGA data analysis (7,8) that the apparent activation energy for cellulose decomposition is similar to that for tar formation.

Olefins and other hydrocarbon gases were not detected in the pyrolysis gases. This is not surprising since these fuels are not products of primary cellulose pyrolysis (12,13). The significant yields of olefins and hydrocarbon gases from flash pyrolysis studies are most likely a result of secondary tar decomposition. Cellulose tars start to decompose at about 550°C, and most of these studies were carried out over the temperature range of about 600-800°C. These observations suggest that results from flash pyrolysis studies are dominated by secondary tar decomposition reactions.

#### ACKNOWLEDGMENTS

This work was supported by the U. S. Department of Energy, Division of Biofuels and Municipal Waste Technology, under Contract W-31-109-Eng-38. The authors wish to acknowledge the support and guidance of J. Lazar, EMW Program Manager at ANL, and K. M. Myles, Section Head in the Chemical Technology Division at ANL.

#### REFERENCES

1. J. L. Kuester, Thermal Systems for Conversion of Municipal Solid Waste, Volume 5, Pyrolytic Conversion: A Technology Status Report, Argonne National Laboratory, ANL/CNSV-TM-120 (June 1983).
2. J. E. Helt et al., Pyrolysis of Municipal Solid Waste, Argonne National Laboratory, ANL/CNSV-45 (Dec. 1984).
3. R. J. Evans et al., Atlas of the Primary Pyrolysis Products of Municipal Solid Waste and Selected Constituents, Solar Energy Research Institute, SERI/SP-234-2597 (Oct. 1984).
4. R. J. Evans and T. A. Milne, Mechanisms of Pyrolysis of Municipal Solid Waste--Annual Report, Solar Energy Research Institute, SERI/PR-234-2852 (Nov. 1985).
5. D. H. White et al., Fundamentals of Direct Liquefaction of Municipal Solid Waste in a Semi-Continuous, Microprocessor-Controlled Autoclave, Argonne National Laboratory, ANL/CNSV-TM-180 (Sept. 1986).
6. J. E. Helt et al., Pyrolysis of Municipal Solid Waste: Annual Report July 1984-June 1985, Argonne National Laboratory, ANL/CNSV-54 (July 1986).
7. J. E. Helt and R. K. Agrawal, Pyrolysis of Municipal Solid Waste Components, AIChE Mtg., Chicago, IL (Nov. 1985).
8. R. K. Agrawal and J. E. Helt, Applications of Thermogravimetry in Energy from Solid Waste Research, 15th Annual North American Thermal Analysis Society Conference, Cincinnati, OH (Sept. 1986).

9. Personal communication Doug Elliot, Pacific Northwest Laboratory, Richland, WA.
10. R. K. Agrawal et al., J. Anal. Appl. Pyrol. 6, 325 (1984).
11. F. Shafizadeh et al., AIChE Symp. Ser. 75, 24 (1979).
12. M. J. Antal, Jr., Adv. Solar Ener. 2, 61 (1983).
13. F. Shafizadeh, J. Anal. Appl. Pyrol. 3, 283 (1982).

Table 1. Composition Ranges for Several MSW Samples<sup>a</sup>

Component	Composition Range, wt %
Paper	30-50
Glass	8-10
Metals	7-10
Plastics	1-5
Rubber-Leather	1-3
Wood	1-4
Textiles	1-5
Food Wastes	10-20
Yard Wastes	5-20
Other	1-4

<sup>a</sup>Reference 1.

Table 2. Analytical Results of Feedstock, Tars, and Chars from Whatman No. 1 Paper (heating rate, 5°C/min; final temp., 475°C)

	Feedstock	Tar Product	Char Product
Heating Value, <sup>a</sup> cal/g	4170	4330	7566
Ash Content, wt %	0.074	-0.075	0.63
Moisture Content, wt %	4.1	--	--
Elemental Analysis, <sup>a</sup> wt %			
Carbon	44.7	42.3(43.6) <sup>b</sup>	81.0(27.3)
Hydrogen	5.9	6.1(47.5)	3.6(10.0)
Oxygen <sup>c</sup>	49.4	51.6(48.0)	15.4(4.7)
Yield, wt %	--	-46	-15

<sup>a</sup>Dry basis.

<sup>b</sup>Numbers in parentheses give percent of original material (based on the reported yields).

<sup>c</sup>Determined by adding together the carbon and hydrogen contents and subtracting them from 100%.

Table 3. Analytical Results of Feedstock, Tars, and Chars from Newsprint (heating rate, 5°C/min; final temp., 475°C)

	Feedstock	Tar Product	Char Product
Heating Value, <sup>a</sup> cal/g	4722	5573	7866
Ash Content, wt %	.95	--	4.1
Moisture Content, wt %	8.3	--	--
Elemental Analysis, <sup>a</sup> wt %			
Carbon	48.0	47.5(45.5) <sup>b</sup>	78.0(24.4)
Hydrogen	5.4	5.6(47.7)	3.7(10.3)
Oxygen <sup>c</sup>	46.6	46.9(46.3)	18.3(5.9)
Yield, wt %	--	-46	-15

<sup>a</sup>Dry basis.

<sup>b</sup>Numbers in parentheses give percent of original material (based on the reported yields).

<sup>c</sup>Determined by adding together the carbon and hydrogen contents and subtracting them from 100%.

Table 4. Analytical Results of Feedstock, Tars, and Chars from Kraft Paper (heating rate, 5°C/min; final temp., 475°C)

	Feedstock	Tar Product	Char Product
Heating Value, <sup>a</sup> cal/g	4445	5272	7333
Ash Content, wt %	1.3	--	4.3
Moisture Content, wt %	6.1	--	--
Elemental Analysis, <sup>a</sup> wt %			
Carbon	47.5	46.9(24.7) <sup>b</sup>	75.5(38.2)
Hydrogen	5.5	5.3(24.1)	3.9(17.0)
Oxygen <sup>c</sup>	47.0	47.8(25.4)	20.6(10.5)
Yield, wt %	--	-25	-24

<sup>a</sup>Dry basis.

<sup>b</sup>Numbers in parentheses give percent of original material (based on the reported yields).

<sup>c</sup>Determined by adding together the carbon and hydrogen contents and subtracting them from 100%.

Table 5. Effect of Sample Weight and Heating Rate on Ultimate Product Yields from Whatman No. 1 Paper

Sample No.	Pyrolysis Sample Weight, g	Heating Rate, °C/min	Yields, %	
			Tar <sup>b</sup>	Char
FPLO8	5	5	46.14	14.55
FFL15	10	5	42.13	15.26
FFL13	15	5	38.54	15.66
FPMD3	5	20	47.18	12.65
FPMD5	5	30	47.76	11.93

<sup>a</sup>Product yields are given for a peak temperature of 475°C.

<sup>b</sup>Based on weight percent Whatman No. 1 paper (dry basis).

Table 6. Effect of Sample Weight and Heating Rate on the Composition of Chars from Whatman No. 1 Paper

Sample No.	Pyrolysis Sample Weight, g	Heating Rate, °C/min	Ultimate Char Yield <sup>a</sup> at 475°C, wt %	Chars, wt %		
				C	H	O <sup>b</sup>
PFL08	5	5	14.55	81.80	3.75	13.45
PFL15	10	5	15.26	81.00	3.55	15.45
PFL13	15	5	15.66	81.90	3.45	14.65
PFPO3	5	20	12.65	81.30	3.45	15.15
PFPO5	5	30	11.93	80.30	3.55	16.15

<sup>a</sup>Yield from original Whatman No. 1 (dry basis).

<sup>b</sup>Derived by adding together C and H contents and subtracting from 100%.

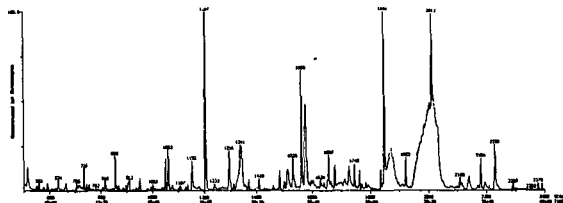


Fig. 1. Mass Spectrum Obtained from Sample 06298402

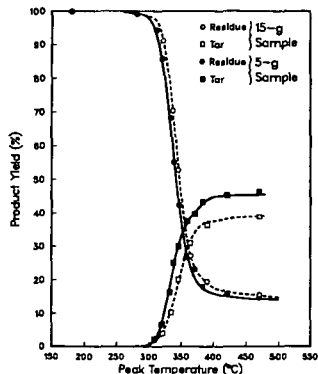


Fig. 2. Effect of Sample Weight on Product Yield for Whatman No. 1 Paper (heating rate, 5°C/min).

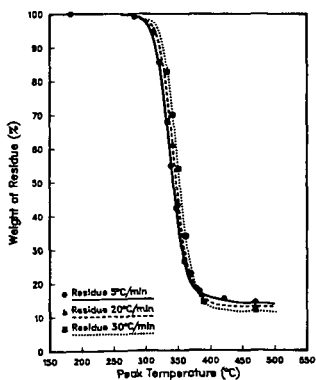


Fig. 3. Effect of Heating Rate on Weight Loss for Whatman No. 1 Paper

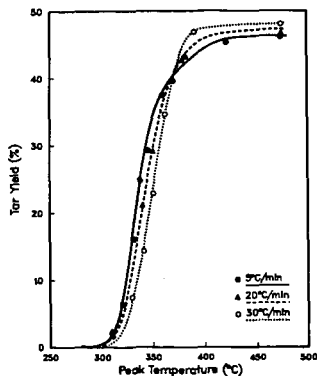


Fig. 4. Effect of Heating Rate on Tar Yields for Whatman No. 1 Paper